

Euclidean mirrors and first-order changepoints in network time series*

Tianyi Chen[†], Zachary Lubberts[‡], Avanti Athreya[§], Youngser Park[¶], and Carey E. Priebe^{||}

Abstract. We describe a model for a network time series whose evolution is governed by an underlying stochastic process, known as the latent position process, in which network evolution can be represented in Euclidean space by a curve, called the Euclidean mirror. We define the notion of a first-order changepoint for a time series of networks, and construct a family of latent position process networks with first-order changepoints. We prove that a spectral estimate of the associated Euclidean mirror localizes these changepoints, even when the graph distribution evolves continuously, but at a rate that changes. Simulated and real data examples on brain organoid networks show that this localization captures empirically significant shifts in network evolution.

Key words. Euclidean mirrors, time series of networks, changepoint localization.

MSC codes. 62F10: Point estimation, 62J05: Linear regression, 62M15: Spectral analysis

1. Introduction. Identifying structural changes for a time series of network data is a critical inference task in modern statistics and interdisciplinary data science. For example, in organizational networks, statistical changepoint detection can identify transformations induced by the COVID-19 pandemic in communication patterns of corporations [35]. In brain organoid networks, changepoint detection can distinguish the biologically significant emergence of inhibitory neurons and growth of astrocytes [6]. As another illustration, spectral network analysis can discern marked fluctuations in global commodity prices in a time series of agricultural trade networks [32]. In all of these cases, the data is a collection of time-indexed networks, each comprised of nodes and edges. The analysis of such time series requires tractably modeling network evolution and managing the inherently non-Euclidean nature of network data.

This non-Euclidean structure, along with the dependency between edges within and across networks, as well as the high dimensionality and noise that accompany Euclidean representations of network features, all present challenges for the development of principled methodology for network time series. As a consequence, while changepoint analysis for Euclidean data has a rich history [24, 4, 12, 29, 19], time series analysis for networks is comparatively new. A natural point of departure is the spectral analysis of a sequence of adjacency matrices or a network tensor: see [21, 10, 20, 15, 32, 2, 1, 18, 14] for approaches to the estimation of common

*Submitted to the editors Sep 2024.

Funding: This work was supported by National Science Foundation (SES-1951005), Office of Naval Research (ONR) Award Number N00024-22-D-6404 (through JHU Applied Physics Laboratory), Office of Naval Research SoA: N00014-24-1-2278, the Amazon-JHU AI2AI Initiative, Microsoft Research, the Acheson J. Duncan Fund for the Advancement of Research in Statistics.

[†]Department of Applied Math and Statistics, Johns Hopkins University, Baltimore, MD (tchen94@jh.edu).

[‡]Corresponding Author. Department of Statistics, University of Virginia, Charlottesville, VA (zlubberts@virginia.edu).

[§]Department of Applied Math and Statistics, Johns Hopkins University, Baltimore, MD (dathrey1@jh.edu).

[¶]Center for Imaging Science, Johns Hopkins University, Baltimore, MD (youngser@jh.edu).

^{||}Department of Applied Math and Statistics, Johns Hopkins University, Baltimore, MD (cep@jh.edu).

parameters, hypothesis testing for differences in networks, and analyses of changepoints and anomalous behavior across networks.

To formalize these ideas, we consider a collection of random networks on the same vertex set, indexed by time. For this network time series, we assume that associated to each vertex i in each network at time t is a (typically unobserved) low-dimensional vector, called the *latent position*, and that the probability of connections between nodes in the network depends on these latent positions. We assume these latent positions evolve according to some underlying stochastic process, called a *latent position process* (LPP). A central question is whether statistical analysis of observed network data can identify changes in the latent position process.

This observed network data consists of a time-indexed collection of adjacency matrices, each entry of which is a Bernoulli random variable with success probability determined by the latent positions of the respective nodes. The observed network adjacency A_t at time t is a noisy version of the matrix of connection probabilities P_t at time t . The matrix of connection probabilities P_t is itself a compression of the information in the realizations of the latent position processes. We do not observe the P_t matrices, much less the realizations of the latent position process. However, because the edge distribution of a latent position network is governed by the LPP, changepoints for the distribution of the network can be associated to changepoints in the latent position process. Specifically, we consider changes in the distribution of the process itself, which we call *zeroth* order changepoints, as well as changepoints in the distribution of the increments of the process, which we term *higher-order changepoints*. We argue that for real-world networks, evolution in the connection probabilities is the norm, rather than the exception, so the appropriate notion of a changepoint should not be merely a change in the network’s distribution, but rather a change in its pattern of evolution. The relevant inference task, then, is to detect if and when such a change in evolution occurs. This phenomena is subtler than previous methodologies have sought to elucidate.

To localize higher-order changepoints, we follow the methodology in [2], where the authors develop a model for time series of networks generated by an LPP and associate to this LPP a finite-dimensional Euclidean curve, called a *mirror*, which provides a Euclidean representation for the network evolution over time. In [2], spectral decompositions and classical multidimensional scaling (CMDS) on the observed time series of networks provide consistent estimates of this mirror. When the mirror exhibits manifold structure, nonlinear dimension reduction techniques, such as isometric mapping (ISOMAP) [27], yield approximations to this manifold, which we dub the *iso-mirror*. The mirror and iso-mirror represent important features of the LPP and the dynamics of the time series of networks, and shifts in the mirror or iso-mirror can reflect corresponding changes in the latent position process.

Figure 1.1 showcases two real data examples from [2] and [6], with plots of iso-mirrors over time. We observe that in both cases, the iso-mirrors exhibit approximate piecewise linearity. The left panel is the iso-mirror for a time series of communication networks at Microsoft during the initial months of pandemic-induced remote work. A notable linear trend is evident before a significant shift around June 2020 [35]. Similarly, the right panel shows the iso-mirror of inferred effective connectivity for brain organoid connectomes. It too displays a piecewise linear trend with a change in the slope at day 188 [6], which coincides with the development of inhibitory neurons and the growth of astrocytes.

Motivated in part by this piecewise linearity, we construct a latent position process net-

work with an asymptotically piecewise linear mirror and a first-order changepoint. The LPP is based on a random walk and the first-order changepoint is introduced by shifting the jump probability at t^* from p to a different value $q \neq p$. We prove that the associated mirror converges uniformly, as the number of networks in our times series increases, to a piecewise linear function with a slope change—namely, a higher-order changepoint—at t^* . Therefore, the task of identifying changepoints within network time series translates to analyzing slope changes in the mirror, allowing us to frame changepoint detection in networks as a changepoint analysis problem in Euclidean space. The asymptotic piecewise linearity property of the mirror leads to a localization estimator for t^* , and we prove that this estimator is consistent. We demonstrate this localization procedure on simulated and real data, and show that networks can differ markedly before and after these higher-order changepoints. Higher-order changepoint localization thus enables the discovery of finer changes in network evolution.

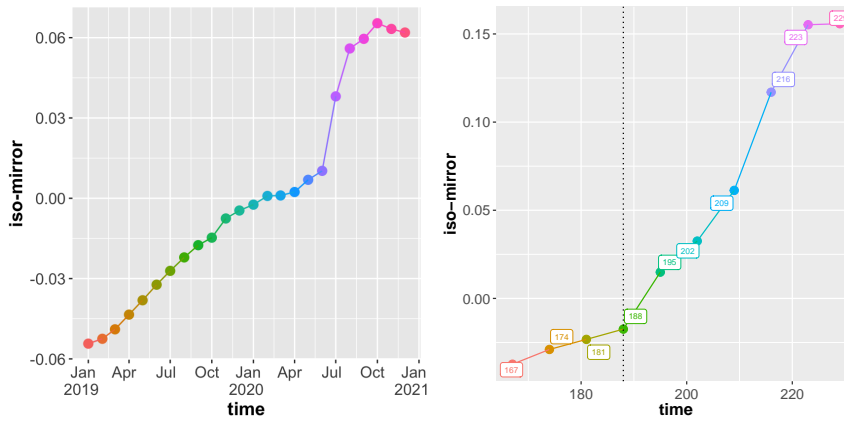


Figure 1.1. Piecewise linearity in a real data example, reproduced from [2]. Left panel shows the iso-mirror estimation for a time series of organizational communication networks generated each month from January 2019 to January 2021. A linear trend observed prior to April 2020, after which COVID-19 work-from-home protocols were introduced. Right panel shows iso-mirror estimation on time series of brain organoid connectivity networks sampled roughly once per week. Estimated iso-mirror exhibits piecewise linearity with slope change at day 188.

1.1. Comparison to previous work. Latent position network models [11, 32, 18, 1, 2, 13] are a common point of departure for both individual and joint network analysis. These include the stochastic block model [3, 18, 8], the generalized random dot product graph, and more intricate latent space models, such as multiplex and multilayer models [15, 32, 11, 22, 17]. In network time series, in addition to a generative model for the network at each time point, it is necessary to describe the dependence between networks at different time points. In [15, 11, 32, 14], the authors propose shared structural framework for the latent positions of nodes across different layers and times. In [15], the latent position matrix for each layer or time is split into initial columns representing common latent positions and subsequent columns for individual latent positions that differ across layers or times. In [14], the authors use kernel debiased sum-of-squares spectral decompositions to estimate community memberships in stochastic blockmodels where block memberships of can shift randomly with time. In [32],

the authors consider a multilayer random dot product model where all layers or times share identical latent positions, but the connectivity matrices determining connection probabilities from these latent positions are allowed to vary. In [18], the authors model inter-network dependence by setting the latent positions $X_i(t)$ for a node i at time t as

$$X_i(t) \begin{cases} = X_i(t-1), & \text{with probability } p, \\ \sim F, & \text{with probability } 1-p, \end{cases}$$

where F is the distribution for the latent position at $t-1$. In [13], a multi-layer perceptron (MLP) is employed to produce a latent position matrix at each time t from a normal distribution $\mathcal{N}(\mu_t, I_d)$, with MLP parameters shared across time. Additionally, several studies assume independence of networks across layers or times [31, 3].

To appropriately model changepoints in network time series, we must delineate how network dynamics evolve over time and investigate different types of changepoints; this motivates our definition of changepoints of different orders. As a baseline model (see [31, 18, 32, 13]) consider what we define as a *zeroth-order* changepoint:

Model 1.1 (Zeroth-order Changepoint). The time series of graphs $\{\mathbf{G}_t\}_{t=1}^m$ having distributions $\{\mathcal{L}_t\}_{t=1}^m$ has a *zeroth-order changepoint* at t^* , $1 < t^* < m$, when

$$\mathcal{L}_{t-1} \neq \mathcal{L}_t \text{ if and only if } t = t^*.$$

In [31], the underlying probability matrices change only at the changepoints; the authors address detection and localization of an unknown number of changepoints and introduce two methods, both relying on cumulative sum (CUSUM) statistics that necessitate dividing the time series data into two separate series. The authors show that under certain conditions, these methods achieve minimax optimality. Similarly, [18] concerns a model where the latent position distribution again changes solely at the changepoints, and the authors deploy spectral methods and CUSUM statistics for localization. In [32], changepoints in multilayer random dot product models are zeroth order, namely time points where the connectivity matrices change. The authors develop techniques for online changepoint detection using scan statistics derived from tensor decompositions of the adjacency matrices in the network time series. In [13], a changepoint is defined as a shift in the expected value μ_t of the distribution generating the latent position matrix. The authors determine $\hat{\mu}_t$ using maximum approximate likelihood estimation, incorporating group-fused lasso regularization, and show that careful analysis of the sequential differences $\hat{\mu}_t - \hat{\mu}_{t-1}$ can effectively detect and localize changepoints.

Here, we consider a time series of networks in which each network is a random dot product graph on the same vertex set with latent positions belonging to the same low-dimensional Euclidean space. We assume the latent positions are samples from a latent position process, with the distributions of these latent positions being dependent across time. A distinctive aspect of our model is that it permits the underlying distribution for networks to drift at each time, with the *rate* of drift altering at the changepoint; this is what we formally define as a first-order changepoint in Section 2. This model renders the algorithms from aforementioned work less effective in localizing our changepoint. Nevertheless, our spectrally-derived estimates of the associated Euclidean mirror for this network time series capture essential signal in the latent position process and lead to intuitive and consistent changepoint localization.

1.2. Organization of paper. We organize the paper as follows. In [Section 2](#), we first introduce our model for network time series; second, we construct a latent position process with a first-order changepoint based on a random walk with a shift in jump probability at a certain time point t^* ; and third, we prove that its associated mirror exhibits an asymptotic piecewise linear structure, with a slope change at t^* . In [Section 3](#) we use spectral techniques and classical multidimensional scaling, both of which require a choice of embedding dimension, to estimate the mirror based on network observations, and we exploit the asymptotic piecewise linearity of the underlying mirror to construct an l_∞ localization estimator for the changepoint t^* . We prove that when asymptotic piecewise linearity holds, this changepoint localization is consistent. In numerical experiments, we demonstrate that the estimated iso-mirror can recover the changepoint, even with a limited sample size n . We also investigate the bias-variance tradeoff in changepoint estimation arising from the choice of embedding dimension for the estimated mirror. Finally, we examine a real data time-series of brain organoid networks, observing a piecewise linear structure for mirror estimates in this data as well, and localizing a changepoint. In [Section 4](#), we discuss ongoing research and further work. All proofs are in the supplementary material.

2. Main model and prior results.

2.1. Notation. Consider a vector $v \in \mathbb{R}^d$, which is represented as a column vector. We express v as $v = (v_1, v_2, \dots, v_d)^\top = [v_i]_{i=1}^d$, where v_i denotes the i th entry of v or sometimes we also use $v(i)$ to denote the i th entry of v . The vector Euclidean norm is denoted by $\|\cdot\|$. For a matrix $A \in \mathbb{R}^{p_1 \times p_2}$, the element at the i, j th position is represented as $(A)_{i,j}$, and A can also be denoted by $[a_{ij}]_{i=1, j=1}^{p_1, p_2}$ with a_{ij} as the i, j th entry. The spectral norm of A is denoted by $\|A\|_2$, the Frobenius norm by $\|A\|_F$, the maximum Euclidean row norm by $\|A\|_{2 \rightarrow \infty}$, and the maximum absolute row sum by $\|A\|_\infty$. For a square matrix $A \in \mathbb{R}^{n \times n}$ with real eigenvalues, $\lambda_1(A)$ denotes the largest eigenvalue, $\lambda_2(A)$ the second largest eigenvalue, and so on. We use Ω to denote a sample space, \mathcal{F} a σ -algebra of events, and \mathbb{P} a probability measure.

We require the following definitions on asymptotic order and convergence.

Definition 2.1 (Order notation). When $\omega(m)$, $\alpha(m)$ are two quantities depending on m , we say that ω is of order $\alpha(m)$ and use the notation $\omega(m) \sim \Theta(\alpha(m))$ if there exist positive constants such that for m sufficiently large, $c\alpha(m) \leq \omega(m) \leq C\alpha(m)$. We write $\omega(m) \sim O(\alpha(m))$ if there exists a constant C such that for sufficiently large m , $\omega(m) \leq C\alpha(m)$.

Definition 2.2 (Convergence with high probability). Given a sequence of events $\{F_n\} \in \mathcal{F}$, where $n = 1, 2, \dots$, we say that F_n occurs with high probability, and write F_n w.h.p., if for some $r > 1$, there exists a finite positive constant C depending on r such that $\mathbb{P}[F_n^c] \leq Cn^{-r}$ for all n .

2.2. Model formulation and key definitions. In our model for network evolution, we build on the framework for network time series in [\[2\]](#) and consider generalized random dot product graphs (GRDPG), which are sufficiently flexible to approximate most independent-edge networks (see [\[26\]](#) and [\[33\]](#)).

Definition 2.3 (Random dot product graph). We say that the undirected random graph G with adjacency matrix $\mathbf{A} \in \mathbb{R}^{n \times n}$ is a random dot product graph (RDPG) with latent position

matrix $\mathbf{X} \in \mathbb{R}^{n \times d}$, whose rows are the vectors $X^1, \dots, X^n \in \mathcal{X} \subseteq \mathbb{R}^d$, if

$$\mathbb{P}[\mathbf{A}|\mathbf{X}] = \prod_{i < j} \langle X^i, X^j \rangle^{A_{i,j}} (1 - \langle X^i, X^j \rangle)^{1-A_{i,j}},$$

where $\langle x, y \rangle = x^\top y$ is the inner product between two column vectors. We call $\mathbf{P} = \mathbf{X}\mathbf{X}^\top$ the connection probability matrix. If instead $\mathbf{P} = \mathbf{X}I_{p,q}\mathbf{X}^\top$, where $I_{p,q} = I_p \oplus (-I_q)$ for some $p+q=d$, we call \mathbf{A} a generalized random dot product graph (GRDPG).

Remark 2.4 (Orthogonal nonidentifiability in RDPGs). Note that if $\mathbf{X} \in \mathbb{R}^{n \times d}$ is a latent position matrix and $\mathbf{W} \in \mathbb{R}^{d \times d}$ is orthogonal, \mathbf{X} and $\mathbf{X}\mathbf{W}$ give rise to the same distribution over graphs. Thus, the RDPG model has a nonidentifiability up to orthogonal transformation. In the case of a GRDPG, \mathbf{X} and $\mathbf{X}\mathbf{W}$ give rise to the same distribution whenever $\mathbf{W}I_{p,q}\mathbf{W}^\top = I_{p,q}$, meaning that \mathbf{W} is an indefinite orthogonal transformation.

To model randomness in the underlying features of each vertex, we consider latent positions that are themselves random variables defined on a probability space $(\Omega, \mathcal{F}, \mathbb{P})$. The notion of an inner product distribution ensures well-defined probabilities.

Definition 2.5 (Inner product distribution). Let F be a probability distribution on \mathbb{R}^d . We call F a d -dimensional inner product distribution if $0 \leq x^\top y \leq 1$ for all $x, y \in \text{supp } F$. We call F a (p, q) -dimensional generalized inner product distribution if $0 \leq x^\top I_{p,q}y \leq 1$ for all $x, y \in \text{supp } F$, where $I_{p,q} = I_p \oplus (-I_q)$.

Suppose that the time series of networks come from an RDPG model, where at each time t , the latent positions of each vertex are drawn independently from a common distribution F_t . To describe such a family of networks indexed by time, we consider a *latent position stochastic process* and its corresponding time series of networks.

Definition 2.6 (Latent position process). A latent position process $\varphi(t)$ is a map $\varphi : [0, T] \rightarrow L^2(\Omega, \mathbb{P})$ such that for each $t \in [0, T]$, $\varphi(t) = X_t$, a random vector in \mathbb{R}^d which has a (generalized) inner product distribution.

Definition 2.7 (Latent position process network time series). Let φ be a latent position process, and fix a given number of vertices n and collection of times $\mathcal{T} \subseteq [0, T]$. We draw an i.i.d. sample $\omega_j \in \Omega$ for $1 \leq j \leq n$, and obtain the latent position matrices $\mathbf{X}_t \in \mathbb{R}^{n \times d}$ for $t \in \mathcal{T}$ by appending the rows $X_t(\omega_j)$, $1 \leq j \leq n$. The time series of graphs (TSG) $\{G_t : t \in \mathcal{T}\}$ are conditionally independent RDPGs with latent position matrices $\mathbf{X}_t, t \in \mathcal{T}$.

Existing literature on changepoint detection for networks has primarily focused on the marginal distributions of the networks. On the other hand, for a TSG where edges are assumed to arise conditionally independently (at each time and between times), and with a fixed small rank d (or p, q with $p+q=d$) for the mean matrices at each time, there is implicitly a (generalized) latent position process governing network evolution. As such, it is natural to define changepoints through properties of the LPP, rather than the distributions of the graphs themselves. This leads us to the notion of changepoints of different orders, below.

Definition 2.8. A latent position process $\varphi(t)$ is said to have a zeroth-order changepoint if

there is some $t^* \in [0, T]$ such that

$$X_t - X_{t'} \stackrel{\mathcal{L}}{=} \begin{cases} \delta_0 & \text{if } t, t' \leq t^* \text{ or } t^* \leq t, t' \\ F \neq \delta_0 & \text{otherwise.} \end{cases}$$

Here δ_0 is point mass at $0 \in \mathbb{R}^d$, and F is some other distribution on \mathbb{R}^d .

Given a partition of $[0, T]$ of mesh δ , define the k th order difference of φ at mesh $\delta > 0$ recursively as follows:

$$\begin{aligned} \Delta_1^\delta(t) &= X_t - X_{t-\delta}, \\ \Delta_k^\delta(t) &= \Delta_{k-1}^\delta(t) - \Delta_{k-1}^\delta(t - \delta). \end{aligned}$$

A latent position process $\varphi(t)$ is said to have a k th-order changepoint of mesh δ if there is some $t^* \in [0, T]$ such that for some distributions $F_1, F_2, F_3(t)$, $t^* < t \leq t^* + \delta$, not all equal, we have

$$\Delta_k^\delta(t) \stackrel{\mathcal{L}}{=} \begin{cases} F_1 & \text{if } t \leq t^*, \\ F_2 & \text{if } t^* + \delta < t, \\ F_3(t) & \text{if } t^* < t \leq t^* + \delta. \end{cases}$$

Note that a first-order changepoint exactly corresponds to the setting in which

$$\{\varphi(t) : t \in [0, t^*)\}, \{\varphi(t) : t \in (t^* + \delta, T]\}$$

are stationary stochastic processes (at least with respect to increments of length δ), but with a loss of stationarity at the point t^* .

We emphasize in [Definition 2.7](#) that each vertex in the TSG corresponds to a single $\omega \in \Omega$, which induces dependence between the latent positions for that vertex across times, but the latent position trajectories of any two distinct vertices are independent of one another across all times. Since these trajectories form an i.i.d. sample from the latent position process, it is natural to measure their evolution over time using the metric on the corresponding random variables, as described in [\[2\]](#). We reproduce the maximum directional variation metric, d_{MV} , a metric on the space of square-integrable random variables, as follows.

Definition 2.9. The maximum directional variation metric $d_{MV} : L^2(\mathbb{R}^d)^2 \rightarrow [0, +\infty)$ is given by

$$(2.1) \quad d_{MV}(X_t, X_{t'}) := \min_{W \in \mathcal{O}^{d \times d}} \left\| \mathbb{E}[(X_t - WX_{t'})(X_t - WX_{t'})^\top] \right\|_2^{1/2},$$

where $\mathcal{O}^{d \times d}$ is the set of all $d \times d$ orthogonal matrices and $\|\cdot\|_2$ is the spectral norm.

In the definition of this distance, the expectation is over $\omega \in \Omega$, which means that it depends on the joint distribution of X_t and $X_{t'}$. In particular, d_{MV} depends on more than just the marginal distributions of the random vectors X_t and $X_{t'}$ individually; it also takes into account the dependence inherited from the latent position process φ .

Next we consider the geometric properties of the image $\varphi([0, T])$ when equipped with the metric d_{MV} . Often, the map φ admits a Euclidean analogue, called a *mirror*, which is a finite-dimensional curve that retains important signal from the generating LPP for the network time series.

Definition 2.10 (Exact Euclidean realizability with mirror ψ). Let φ be a latent position process. We say that the LPP φ is exactly Euclidean c -realizable with mirror ψ if there exists a Lipschitz continuous curve $\psi : [0, T] \rightarrow \mathbb{R}^c$ such that:

$$d_{MV}(\varphi(t), \varphi(t')) := d_{MV}(X_t, X_{t'}) = \|\psi(t) - \psi(t')\| \text{ for all } t, t' \in [0, T].$$

Remark 2.11. Exact Euclidean realizability implies the pairwise d_{MV} distances between the latent position process at t and t' coincide exactly with Euclidean distances along the curve ψ at t and t' . This curve reflects, in Euclidean space, the d_{MV} distances, and hence we call ψ the *Euclidean mirror*.

We similarly define approximate Euclidean realizability.

Definition 2.12 (Approximate Euclidean realizability with mirror ψ). Let φ be a latent position process. For a fixed $\alpha \in (0, 1)$, we say that φ is approximately α -Hölder Euclidean c -realizable if ψ is α -Hölder continuous, and there is some $C > 0$ such that

$$\left| d_{MV}(\varphi(t), \varphi(t')) - \|\psi(t) - \psi(t')\| \right| \leq C|t - t'|^\alpha \text{ for all } t, t' \in [0, T].$$

If the LPP is exactly c -Euclidean realizable with mirror ψ , and we sample m time points

$$\mathcal{T} = \{t_1, t_2, \dots, t_m\} \subseteq [0, T],$$

then the corresponding distance (or dissimilarity) matrix

$$(\mathcal{D}_\varphi)_{i,j} := d_{MV}(X_{t_i}, X_{t_j})$$

is an *exactly c -Euclidean realizable distance (dissimilarity) matrix*: that is, there exist m points

$$\psi(t_1), \psi(t_2), \dots, \psi(t_m) \in \mathbb{R}^c$$

such that

$$(\mathcal{D}_\varphi)_{i,j} = \|\psi(t_i) - \psi(t_j)\| \text{ for all } i, j \in \{1, 2, \dots, m\}.$$

In this case, applying classical multidimensional scaling (CMDS) to \mathcal{D}_φ will recover the mirror $\psi(t_1), \psi(t_2), \dots, \psi(t_m)$ exactly up to an orthogonal transformation. Recall that the CMDS embedding is defined as follows.

Definition 2.13 (CMDS embedding to dimension c). Let $\mathcal{D} \in \mathbb{R}^{m \times m}$ be a distance matrix and define the centering matrix P by $P := I_m - \frac{J_m}{m}$ where I_m is the $m \times m$ identity matrix and J_m is the $m \times m$ all ones matrix. Consider $B := -\frac{1}{2}P\mathcal{D}^{(2)}P$ where $\mathcal{D}^{(2)}$ is the entrywise square of the distance matrix \mathcal{D} . Denote the c largest eigenvalues and corresponding orthogonal eigenvectors of B as $\lambda_1, \dots, \lambda_c$ and u_1, \dots, u_c . Set $\max(\lambda_i, 0) = \sigma_i^2$ and S a diagonal matrix with $S_{ii} := \sigma_i^2$ for $i \in \{1, \dots, c\}$; let $U \in \mathbb{R}^{m \times c} := [u_1 | \dots | u_c]$. The classical multidimensional scaling of \mathcal{D} into dimension c , where $1 \leq c \leq m-1$, is the set of m points $\psi(t_1), \dots, \psi(t_m) \in \mathbb{R}^c$ defined by the rows of Ψ as

$$\Psi := [\psi_j(t_i)]_{i=1, j=1}^{m,c} = \begin{bmatrix} \psi_1(t_1) & \cdots & \psi_c(t_1) \\ \vdots & & \vdots \\ \psi_1(t_m) & \cdots & \psi_c(t_m) \end{bmatrix} = \begin{bmatrix} \psi^\top(t_1) \\ \vdots \\ \psi^\top(t_m) \end{bmatrix} = US^{\frac{1}{2}} = [\sigma_1 u_1 | \cdots | \sigma_c u_c].$$

Remark 2.14. If there are no positive eigenvalues for B , then $S = 0$ and thus $\Psi = 0$. This implies that the distance matrix has no meaningful Euclidean representation. As highlighted in [Theorem 2.15](#), B must be positive semidefinite for \mathcal{D} to be exactly Euclidean realizable.

The next theorem from [28] gives necessary and sufficient conditions for a distance matrix to be exactly Euclidean realizable.

Theorem 2.15. *A distance matrix \mathcal{D} is exactly c Euclidean realizable, and is not $c - 1$ Euclidean realizable, if and only if $B = -\frac{1}{2}P\mathcal{D}^{(2)}P$ is positive semidefinite with exactly c positive eigenvalues.*

Embedding a distance or dissimilarity matrix through CMDS provides a constellation of points in Euclidean space whose interpoint Euclidean distances approximate those in the dissimilarity matrix. In the case of a latent position process, this embedding can provide key signal about the underlying process itself. We call this the *zero-skeleton* mirror.

Definition 2.16 (Zero-skeleton mirror). *Suppose \mathcal{D}_φ is the d_{MV} distance matrix associated with an LPP φ . The output of CMDS applied to \mathcal{D}_φ produces m points in \mathbb{R}^c , denoted $\{\psi(t_1), \dots, \psi(t_m)\}$, called the zero-skeleton c -dimensional (d_{MV}) mirror.*

Remark 2.17. Throughout the paper, $\psi(\cdot) : [0, T] \rightarrow \mathbb{R}^c$, where c is the chosen CMDS embedding dimension, denotes the c -dimensional Euclidean mirror. The image of the function ψ is a c dimensional curve, and $\psi(t) \in \mathbb{R}^c$ provides representation of the graph at time t in c dimensional Euclidean space. When $c > 1$, we use $\psi_k : \mathbb{R} \rightarrow \mathbb{R}$ to denote the k th component of ψ and $[\psi_k(t_i)]_{i=1}^m = \sigma_k u_k$. When we consider m time points, we stack $\{\psi^\top(t_1), \psi^\top(t_2), \dots, \psi^\top(t_m)\}$ row-wise, as a matrix, denoted by $\Psi \in \mathbb{R}^{m \times c}$.

As we have seen in the analysis of TSGs from multiple application domains, the mirror is often approximately 1-d Euclidean realizable and exhibits piecewise linear structure. In the following section, we introduce a class of LPP models which give rise to an analytically computable, asymptotically piecewise linear mirror with a first-order changepoint, and we use spectral decompositions of the observed networks to localize this changepoint. The formal construction of a specific LPP with such piecewise linear structure allows us to develop principled methodology for changepoint localization in these settings.

2.3. Random walk latent position process. In this section, we introduce a simple class of LPPs with a closed-form d_{MV} distance. This enables us to analytically compute the mirror obtained through CMDS.

Model 2.18 (Random walk latent position process). Let m be an integer, $m \geq 2$. Let t be an integer with $0 \leq t \leq m$. Let $c \geq 0, \delta_m > 0$ be two constants satisfying $c + \delta_m m \leq 1$. For a fixed “jump probability” $p \in (0, 1)$, define a LPP φ_m as follows:

$$\begin{aligned} X_0 &= c \quad \text{with probability 1,} \\ \text{For } t \geq 1, \quad X_t &= \begin{cases} X_{t-1} + \delta_m & \text{with probability } p, \\ X_{t-1} & \text{with probability } 1 - p. \end{cases} \end{aligned}$$

We can, of course, express this latent position process as a familiar random walk: let $Z_i, i \geq 1$, be i.i.d random variables defined by $Z_i = \delta_m$ with probability p and $Z_i = 0$ with

probability $1 - p$; let $Z_0 = c$ with probability one. Then for $t \in \{0, 1, 2, \dots, m\}$, $X_t = \sum_{k=0}^t Z_k$. Observe that for $t \geq 1$, $X_t - c = V_t \delta_m$, where V_t is a Binomial random variable with t trials and success probability p . Note that X_t depends on m ; in what follows, we suppress this dependence for notational convenience, but we will consider it in more detail in subsequent sections.

Since $c + \delta_m m \leq 1$, as m increases, δ_m must decrease. For the rest of this section, we consider $X_0 = 0$ and $\delta_m = \frac{1}{m}$ so that our latent position process is supported on the set $\{0, \frac{1}{m}, \dots, 1\}$. (When we consider a time series of graphs, we generally require $c > 0$ and $c + \delta_m m \leq 1$ to ensure sufficient signal strength in each network, but we adopt the specific choice of $c = 0$ and $\delta_m = 1/m$ in the present section for notational simplicity.)

The random dot product graph (RDPG) at time t whose vertices have latent positions distributed according to X_t is actually an $(m + 1)$ -block stochastic block model (SBM) with block assignment vector $\pi_{t,m,p}$ and block connection probability matrix B_m defined by

$$\pi_{t,m,p}(i) = \begin{cases} \binom{t}{i} p^i (1-p)^{t-i} & \text{for } i \in \{0, 1, 2, \dots, t\} \\ 0 & \text{for } i \in \{t+1, t+2, \dots, m\}, \end{cases}$$

$$(B_m)_{i,j} = \frac{ij}{m^2} \quad \text{where } i, j \in \{0, 1, 2, \dots, m\}.$$

Note B_m is a rank one matrix. The d_{MV} distance is analytically tractable for [Model 2.18](#), and we compute it here.

Lemma 2.19. *For these latent position process in [Model 2.18](#),*

$$(2.2) \quad d_{MV}^2(X_t, X_{t'}) = \left(\frac{p(t-t')}{m} \right)^2 + (p-p^2) \frac{|t-t'|}{m^2} \quad \text{for all } t, t' \in \{1, 2, \dots, m\},$$

and this LPP is approximately $\frac{1}{2}$ -Hölder Euclidean 1-realizable with mirror $\psi(t) = \frac{pt}{m}$:

$$(2.3) \quad \left| d_{MV}(X_t, X_{t'}) - \|\psi(t) - \psi(t')\| \right| \leq \sqrt{p-p^2} \frac{|t-t'|^{\frac{1}{2}}}{m} \quad \text{for all } t, t' \in \{1, 2, \dots, m\}.$$

Let $\mathcal{D}_{\varphi_m}^{(2)}$ denote the $m \times m$ matrix of pairwise squared distances whose i, j th entry is given by

$$\left(\mathcal{D}_{\varphi_m}^{(2)} \right)_{i,j} = d_{MV}^2(X_i, X_j) = p^2 \left(\frac{i}{m} - \frac{j}{m} \right)^2 + \frac{p-p^2}{m} \left| \frac{i}{m} - \frac{j}{m} \right| \quad \text{where } i, j \in \{1, 2, \dots, m\}.$$

An important consequence of [Lemma 2.19](#) is that the d_{MV} distance in [\(2.2\)](#) is the sum of two terms, the first of which is quadratic in the difference between i/m and j/m , and the second of which involves the absolute value of the difference between i/m and j/m , scaled by an additional factor of $1/m$. Consider the case in which $i/m \rightarrow x$ and $j/m \rightarrow y$ as $m \rightarrow \infty$. Here, the second term in the d_{MV} distance is of order $1/m$, but the first term is of constant order, making it the dominant term in the sum. As mentioned above, the first term, a quadratic in the distance between i/m and j/m , is the square of a 1-dimensional Euclidean

distance. Hence for large m , we expect that classical multidimensional scaling applied to this dissimilarity will yield, in the first dimension, an approximately linear curve. To illustrate this, we show in Figure 2.1 the CMDS results for the first three dimensions, plotted against the time increment m , with model parameters $c = 0.1$, $\delta = \frac{0.9}{m}$, and $m = 40$, $p = 0.4$. The black dots are the output of CMDS on the true distance matrix \mathcal{D}_{φ_m} .

Clearly the first dimension of the mirror is close to the linear function $\psi(t) = p(\frac{t}{m} - \frac{1}{2})$ after centering. The second and third dimensions, by contrast, are sinusoidal, but range over an order-of-magnitude smaller scaling: these serve to approximate the diminishing absolute value of the differences encapsulated in the second term of the d_{MV} distance.

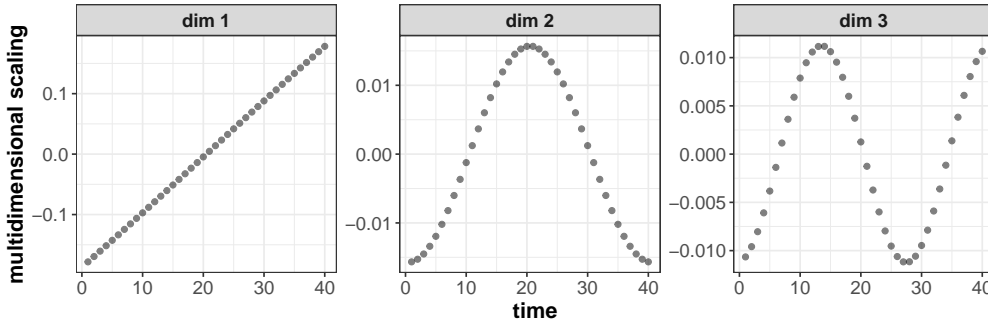


Figure 2.1. The first three dimensions of CMDS for the true distance matrix \mathcal{D}_{φ_m} for Model 2.18, where $c = 0.1$, $\delta = \frac{0.9}{m}$, and $m = 40$, $p = 0.4$. The left panel, the first dimension of CMDS, shows an approximately linear function of time increments m . The second and third dimensions, by contrast, are sinusoidal, but range over an order-of-magnitude smaller scaling. We describe this in further detail in the supplement.

2.4. Random walk latent position process with first-order changepoint. Having found the first dimension of the mirror for the LPP in Model 2.18, we consider adding a changepoint to the LPP at time t^* and examining whether this is effectively captured by the mirror itself, either in terms of localization of t^* or detection of an underlying distributional change. We introduce a more general LPP φ_m which includes Model 2.18 as a submodel, but allows for a first-order changepoint via a modification of the jump probability at t^* .

Model 2.20 (Random walk LPP with first-order changepoint). Let $m \geq 2$ be an integer. Let $c \geq 0, \delta_m > 0$ be constants satisfying $c + \delta_m m \leq 1$. We define the *random walk latent position process with first-order jump probability changepoint at t_m^** by

$$X_0 = c \quad \text{with probability 1,}$$

$$X_t = \begin{cases} X_{t-1} + \delta_m & \text{with probability } p_t \\ X_{t-1} & \text{with probability } 1 - p_t, \end{cases}$$

where $p_t = p$ for $t \leq t_m^*$ and $p_t = q$ for $t > t_m^*$, where $p \neq q$ and $t, t_m^* \in \{1, 2, \dots, m\}$.

Set $c = 0$ and $\delta_m = \frac{1}{m}$; we calculate the d_{MV} distance in this case. Our next lemma exhibits the true d_{MV} distance matrix for this process.

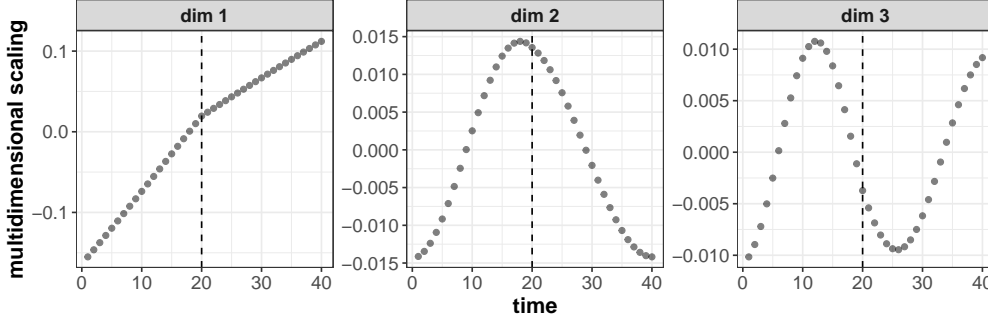


Figure 2.2. The first three dimensions of CMDS for the true distance matrix \mathcal{D}_{φ_m} for *Model 2.20*, where $c = 0.1$, $\delta = \frac{0.9}{m}$, and $m = 40$, $p = 0.4$, $q = 0.2$, and $t_m^* = 20$. The first dimension, given in the leftmost panel, shows approximate piecewise linearity with a slope change at t_m^* . The second and third dimensions also exhibit a change in behavior at t_m^* , where the frequency of the cosine and sine curves changes abruptly, but the range in both sinusoidal terms is an order of magnitude smaller; again, we describe this in further detail in the supplement.

Lemma 2.21. For the latent position process in *Model 2.20*,

$$\left(\mathcal{D}_{\varphi_m}^{(2)}\right)_{i,j} = d_{MV}^2(X_i, X_j) = \begin{cases} p^2 \left(\frac{i}{m} - \frac{j}{m}\right)^2 + \frac{p-p^2}{m} \left|\frac{i}{m} - \frac{j}{m}\right| & i, j < t_m^*, \\ \left(p\left(\frac{t_m^*}{m} - \frac{i}{m}\right) + q\left(\frac{j}{m} - \frac{t_m^*}{m}\right)\right)^2 + \frac{p-p^2}{m} \left|\frac{t_m^*}{m} - \frac{i}{m}\right| + \frac{q-q^2}{m} \left|\frac{j}{m} - \frac{t_m^*}{m}\right| & i < t_m^* < j, \\ q^2 \left(\frac{i}{m} - \frac{j}{m}\right)^2 + \frac{q-q^2}{m} \left|\frac{i}{m} - \frac{j}{m}\right| & t_m^* < i, j. \end{cases}$$

This LPP is approximately $\frac{1}{2}$ -Hölder Euclidean 1-realizable with mirror

$$\psi(t) = \begin{cases} \frac{pt}{m} & \text{for } t \leq t_m^*, \\ \frac{qt}{m} + \frac{(p-q)t_m^*}{m} & \text{for } t > t_m^*, \end{cases}$$

and

$$(2.4) \quad \left|d_{MV}(X_t, X_{t'}) - \|\psi(t) - \psi(t')\|\right| \leq \frac{|t - t'|^{\frac{1}{2}}}{2m} \quad \text{for all } t, t' \in \{1, 2, \dots, m\}.$$

The proof of this lemma is similar to *Lemma 2.19*. As in the case without a changepoint, the absolute value terms in this function are of order $1/m$ as m grows. This leads to a distance that is well-approximated by Euclidean distance along a one-dimensional piecewise linear curve with a change of slope at t_m^* . We devote the next section to the asymptotic behavior of these two models.

2.5. In-fill asymptotics of the mirror. To understand the asymptotics of estimation for latent position processes and associated mirrors as the number of time points m increases, we note that the time points t_1, \dots, t_m are constrained to lie in a fixed bounded interval, but this interval is sampled increasingly often as m increases. As we show, certain latent position processes can converge to deterministic limits as the number of sampled time points increases. The next lemma guarantees that such deterministic latent position processes satisfy exact Euclidean 1-realizability and have explicitly computable mirrors.

Lemma 2.22. *If the latent position process $\{\varphi(t)\}$ is deterministic and $t \in (a, b)$, $\varphi(t) \in \mathbb{R}^d$, then it is exactly Euclidean 1-realizable, with mirror $\psi(t) = \|\varphi(t)\|_2 - \frac{\int_a^b \|\varphi(s)\|_2 ds}{b-a}$.*

We note that for either of these models, as m grows, the discrete time LPP does not append any additional random variables. That is, denoting the LPP with m time-points by $\{X_{t_1}^{(m)}, \dots, X_{t_m}^{(m)}\}$, we have $\{X_{t_1}^{(m)}, \dots, X_{t_m}^{(m)}\} \not\subseteq \{X_{t_1}^{(m+1)}, \dots, X_{t_{m+1}}^{(m+1)}\}$. These are two completely different LPPs and $X_{t_1}^{(m)} \neq X_{t_1}^{(m+1)}$. For example in [Model 2.18](#), for fixed p , after scaling by m , the LPP is determined by the time points $\{t_1, \dots, t_m\} = \{\frac{1}{m}, \dots, 1\}$; thus as m grows, the times change and the points t_k fill the interval $[0, 1]$. For [Model 2.18](#) and [Model 2.20](#), when $m \rightarrow \infty$, the LPP converges in L^2 to a deterministic LPP, as the following lemma formalizes.

Lemma 2.23. *Consider $t_{\beta,m} = \lfloor m\beta \rfloor$ with $\beta \in [0, 1]$ fixed as $m \rightarrow \infty$. Denote by $X_{t_{\beta,m}}^{(m)}$ be the latent position process for [Model 2.18](#), for a given m , evaluated at $t_{\beta,m}$. Let $\{Z_t, 0 \leq t \leq 1\}$ denote the continuous deterministic LPP defined by $Z_t = tp$. Then $X_{t_{\beta,m}}^{(m)} \xrightarrow{L^2} Z_\beta$ for any β as $m \rightarrow \infty$.*

Next, Consider $t_{\beta,m} = \lfloor m\beta \rfloor$ with $\beta \in [0, 1]$ fixed and $t_m^ = \lfloor mt^* \rfloor$ with $t^* \in [0, 1]$ as $m \rightarrow \infty$. Suppose $\tilde{X}_{t_{\beta,m}}^{(m)}$ is the latent position process for [Model 2.20](#) with change of jump probability at t_m^* , for a given m at $t_{\beta,m}$. Define the deterministic latent position process by*

$$Z_\beta = \begin{cases} p\beta & \text{for } \beta \leq t^* \\ q\beta + (p-q)t^* & \text{for } \beta > t^*, \end{cases}$$

where p, q are as in [Model 2.20](#). Then $\tilde{X}_{t_{\beta,m}}^{(m)} \xrightarrow{L^2} Z_\beta$ for any β and t^* as $m \rightarrow \infty$.

By [Lemma 2.22](#), the mirror ψ_Z associated to Z_t is piecewise linear:

$$(2.5) \quad \psi_Z(t) = \begin{cases} pt + c_0 & \text{for } t \leq t^* \\ qt + (p-q)t^* + c_0 & \text{for } t > t^*. \end{cases}$$

$$\text{where } c_0 = t^*(p-q) \left(\frac{t^*}{2} - 1 \right) - \frac{q}{2} \text{ such that } \int_0^1 \psi_Z(t) dt = 0.$$

We now define the notion of *asymptotically exactly Euclidean 1-realizable* LPPs:

Definition 2.24 (In-fill (summably) asymptotically Euclidean 1-realizable). *Consider a latent position process X_t , sampled at $0 \leq t_1 < \dots < t_m \leq 1$ and denoted by $\mathcal{X} = \{X_{t_1}^{(m)}, \dots, X_{t_m}^{(m)}\}$, that is exactly Euclidean $(m-1)$ -realizable with 0-skeleton mirror $\{\psi^{(m)}(t_1), \dots, \psi^{(m)}(t_m)\}$.*

Define $\tilde{\psi}_1^{(m)}$ to be the piecewise linear interpolation between the points $\left\{ \left(t_i, \psi_1^{(m)}(t_i) \right) \right\}_{i=1}^m$. We say the latent position process X_t is asymptotically Euclidean 1-realizable with asymptotic mirror ψ_0 if there exists a function $\psi_0 : [0, 1] \rightarrow \mathbb{R}^1$ such that

$$\sup_{t \in [0,1]} |\tilde{\psi}_1^{(m)}(t) - \psi_0(t)| \rightarrow 0 \text{ as } m \rightarrow \infty,$$

and

$$\left| d_{MV} \left(X_{t_i}^{(m)}, X_{t_j}^{(m)} \right) - |\psi_0(t_i) - \psi_0(t_j)| \right| \rightarrow 0 \text{ as } m \rightarrow \infty \text{ for all } i, j \in \{1, 2, \dots, m\}.$$

Suppose, in addition, that the following conditions hold:

$$\lambda_1 \left(-\frac{1}{2} P \mathcal{D}_m^{(2)} P \right) \sim \Theta(m),$$

$$\frac{\sum_{i=2}^m \lambda_i^2 \left(-\frac{1}{2} P \mathcal{D}_m^{(2)} P \right)}{\lambda_1 \left(-\frac{1}{2} P \mathcal{D}_m^{(2)} P \right)} \sim O \left(\frac{1}{m} \right),$$

where $(\mathcal{D}_m)_{i,j} = d_{MV} \left(X_{t_i}^{(m)}, X_{t_j}^{(m)} \right)$. In this case, we call the latent position process summably asymptotically Euclidean 1-realizable.

An asymptotically Euclidean 1-realizable LPP is such that the first dimension of the mirror uniformly converges to the one-dimensional curve ψ_0 , which asymptotically matches the distances in \mathcal{D}_m ; we can naturally extend this definition to asymptotic Euclidean d -realizability.

Asymptotic realizability is concerned with the behavior, as m increases, of the latent position process defined for the points t_1, \dots, t_m in the unit interval, which is a fixed, bounded interval. Since the number of points t_i in this interval increases, we consider a time rescaling of [Model 2.20](#) with changepoints t_m^* satisfying $t_m^* = \lfloor t^* m \rfloor$ for some fixed $t^* \in (0, 1)$. This leads us to the notion of an *in-fill random walk latent position process with changepoint*.

Model 2.25 (In-fill random walk LPP with changepoint). Let $t^* \in (0, 1)$. For any $m \geq 2$, set $c = 0$, $\delta_m = 1/m$, and let $\tilde{X}_t^{(m)}$ follow the random walk LPP of [Model 2.20](#) with first-order jump probability changepoint at $t_m^* = \lfloor t^* m \rfloor$. Put $t_i = i/m$ for $i \in \{1, \dots, m\}$ and define the *in-fill random walk LPP with changepoint at t^** as

$$X_{t_i}^{(m)} = \tilde{X}_i^{(m)}, 1 \leq i \leq m.$$

That is,

$$X_0^{(m)} = 0 \text{ with probability 1,}$$

$$X_{t_i}^{(m)} = \begin{cases} X_{t_{i-1}}^{(m)} + \frac{1}{m} & \text{with probability } p_{t_i} \\ X_{t_{i-1}}^{(m)} & \text{with probability } 1 - p_{t_i}, \end{cases}$$

where $p_{t_i} = p$ for $t_i \leq t^*$ and $p_{t_i} = q$ for $t_i > t^*$.

Observe that the distance matrix for [Model 2.25](#) is

$$\left(\mathcal{D}_{\varphi_m}^{(2)} \right)_{i,j} = \begin{cases} \frac{p^2}{m^2} (i-j)^2 + \frac{p-p^2}{m^2} |i-j| & i, j < t_m^*, \\ \left(\frac{p}{m} (t_m^* - i) + \frac{q}{m} (j - t_m^*) \right)^2 + \frac{p-p^2}{m^2} (t_m^* - i) + \frac{q-q^2}{m^2} (j - t_m^*) & i < t_m^* < j, \\ \frac{q^2}{m^2} (j-i)^2 + \frac{q-q^2}{m^2} |i-j| & t_m^* < i, j. \end{cases}$$

With ψ_Z as given in Eq. (2.5), we define the squared dissimilarity matrix $\mathcal{D}_Z^{(2)}$ as follows:

$$\left(\mathcal{D}_Z^{(2)}\right)_{i,j} = \left(\psi_Z\left(\frac{i}{m}\right) - \psi_Z\left(\frac{j}{m}\right)\right)^2 = \begin{cases} \frac{p^2}{m^2}(i-j)^2 & i, j < t_m^*, \\ \left(\frac{p}{m}(t_m^* - i) + \frac{q}{m}(j - t_m^*)\right)^2 & i < t_m^* < j, \\ \frac{q^2}{m^2}(i-j)^2 & t_m^* < i, j. \end{cases}$$

As mentioned above, we observe that

$$\left(\mathcal{D}_Z^{(2)} - \mathcal{D}_{\varphi_m}^{(2)}\right)_{i,j} \sim O\left(\frac{1}{m}\right) \quad \text{for all } i, j \in \{1, 2, \dots, m\}.$$

We focus on two main results on changepoint localization. The first, [Theorem 2.26](#), guarantees that as $m \rightarrow \infty$, the changepoint LPP in [Model 2.25](#) is summably asymptotically Euclidean 1-realizable with a piecewise linear asymptotic mirror. The second pair of results, [Theorem 3.10](#) and [Theorem 3.14](#) in [Subsection 3.2](#), show that spectral methods can consistently locate this changepoint. [Theorem 2.26](#), below, asserts that the asymptotic mirror associated for the LPP in [Model 2.25](#) has piecewise linear structure with a change in slope at the LPP changepoint, reinforcing the core idea that the Euclidean mirror (or its asymptotic variant) captures core features of the underlying network evolution.

Theorem 2.26 ([Model 2.25 is summably asymptotically Euclidean 1-realizable with piecewise linear asymptotic mirror](#)). *Consider the in-fill random walk latent position process in [Model 2.25](#) with changepoint at $t^* \in (0, 1)$. This LPP is summably asymptotically Euclidean 1-realizable with asymptotic mirror given by the piecewise linear function ψ_Z :*

$$\psi_Z(t) = \begin{cases} pt + c_0 & \text{for } t \leq t^* \\ qt + (p - q)t^* + c_0 & \text{for } t > t^*. \end{cases}$$

$$\text{where } c_0 = t^*(p - q)\left(\frac{t^*}{2} - 1\right) - \frac{q}{2} \text{ such that } \int_0^1 \psi_Z(t)dt = 0.$$

Namely, the following four properties hold:

- (1) there exist $w_m \in \{\pm 1\}$ such that $\sup_{t \in [0, 1]} |\tilde{\psi}_1^{(m)}(t) - w_m \psi_Z(t)| \rightarrow 0$ as $m \rightarrow \infty$,
- (2) $\max_{i, j \in \{1, 2, \dots, m\}} \left(\mathcal{D}_{\varphi_m}^{(2)} - \mathcal{D}_Z^{(2)}\right)_{i, j} \rightarrow 0$ as $m \rightarrow \infty$,
- (3) $\tilde{\lambda}_1 \sim \Theta(m)$, where $\tilde{\lambda}_1, \tilde{\lambda}_2, \dots, \tilde{\lambda}_m$ are eigenvalues of $-\frac{1}{2}P\mathcal{D}_{\varphi_m}^{(2)}P$,
- (4) $\frac{\sum_{i=2}^m \tilde{\lambda}_i^2}{\tilde{\lambda}_1} \sim O\left(\frac{1}{m}\right)$ as $m \rightarrow \infty$.

This theorem guarantees the piecewise linearity of the asymptotic mirror ψ_Z for the LPP in [Model 2.25](#) and also shows that the jump probability changepoint t^* of the underlying LPP coincides with the slope changepoint in the asymptotic mirror ψ_Z . Next, we use this observation to consistently localize the changepoint from an observed time series of networks coming from such an LPP.

3. Changepoint analysis. In [Model 2.25](#), at the changepoint t^* , the jump probability changes in the LPP itself. As we defined in [Definition 2.8](#), this is a first-order changepoint for the LPP. Indeed, for a fixed m and any $i \in \{1, 2, \dots, m\}$:

$$\Delta_1^{\frac{1}{m}}(t_i) \stackrel{\mathcal{L}}{=} \begin{cases} \frac{1}{m}K_p & \text{if } t_i \leq t^*, \\ \frac{1}{m}K_q & \text{if } t^* + \frac{1}{m} < t_i, \\ \frac{1}{m}K_q & \text{if } t^* < t_i \leq t^* + \frac{1}{m}, \end{cases}$$

where K_p is a Bernoulli random variable with success probability p . In this section, we adapt techniques from [\[2\]](#) to show that network realizations from the in-fill LPP model ([Model 2.25](#)) can be used to estimate Euclidean mirrors and localize changepoints associated to the underlying latent position process.

3.1. Estimation of model parameters from network realizations. Our network time series consists of time-indexed graphs on a common vertex set, and for any given time, each vertex has a corresponding time-dependent latent position. The latent positions are typically unknown, but can be consistently estimated through spectral decompositions of the observed adjacency matrices [\[25\]](#). Suppose that G is a random dot product graph with latent position matrix $\mathbf{X} \in \mathbb{R}^{n \times d}$, where the rows of \mathbf{X} are independent, identically distributed draws from a latent position distribution F on \mathbb{R}^d . Let $\mathbf{P} = \mathbf{X}\mathbf{X}^T$ be the connection probability matrix and \mathbf{A} be the adjacency matrix for this graph. The *adjacency spectral embedding* (ASE) is a rank d eigendecomposition of the adjacency matrix.

Definition 3.1 (Adjacency Spectral Embedding). *Given an adjacency matrix \mathbf{A} , we define the adjacency spectral embedding (ASE) with dimension d as $\hat{\mathbf{X}} = \hat{\mathbf{U}}|\hat{\mathbf{S}}|^{1/2}$, where $\hat{\mathbf{S}} \in \mathbb{R}^{d \times d}$ is the diagonal matrix with the d largest-magnitude eigenvalues of \mathbf{A} on its diagonal, arranged in decreasing order. $\hat{\mathbf{U}} \in \mathbb{R}^{n \times d}$ is the matrix of d corresponding orthonormal eigenvectors arranged in the same order. $\hat{\mathbf{X}}$ is the estimated latent position matrix.*

When the true dimension d of the latent positions—or equivalently, the rank of \mathbf{P} —is unknown, we can infer it using the scree plot [\[34\]](#). The ASEs of the observed adjacency matrices in our TSG at times t and s , denoted $\hat{\mathbf{X}}_t$ and $\hat{\mathbf{X}}_s$, are estimates of the latent position matrices \mathbf{X}_t and \mathbf{X}_s , from which we obtain an estimate \hat{d}_{MV} , defined below, of the d_{MV} distance between the latent position random variables over time.

Definition 3.2. *The estimated d_{MV} distance \hat{d}_{MV} is defined as*

$$(3.1) \quad \hat{d}_{MV}(\hat{\mathbf{X}}_t, \hat{\mathbf{X}}_s) := \min_{W \in \mathcal{O}^{d \times d}} \frac{1}{\sqrt{n}} \|\hat{\mathbf{X}}_t - \hat{\mathbf{X}}_s W\|_2.$$

In [\[2\]](#), the authors show that \hat{d}_{MV} is a consistent estimate for the true dissimilarity.

Theorem 3.3. *[2] With overwhelming probability,*

$$\left| \hat{d}_{MV}(\hat{\mathbf{X}}_t, \hat{\mathbf{X}}_s)^2 - d_{MV}(\varphi(t), \varphi(s))^2 \right| \leq \frac{\log(n)}{\sqrt{n}}.$$

Sampling our network time series at m time points, we obtain m adjacency matrices whose spectral embeddings yield the matrix $\hat{\mathcal{D}}$ of pairwise estimated dissimilarities:

$$\left(\hat{\mathcal{D}}_\varphi \right)_{s,t} = \hat{d}_{MV}(\hat{\mathbf{X}}_s, \hat{\mathbf{X}}_t).$$

As in [Definition 2.13](#), let $P := I_m - \frac{J_m}{m}$ where I_m is the $m \times m$ identity matrix and J_m is the $m \times m$ all ones matrix. Recall from [Definition 2.16](#) that the c -dimensional zero-skeleton mirror ψ for the latent position process φ is given by the rows of $US^{1/2}$, where S is the diagonal matrix of the c largest positive eigenvalues of $-\frac{1}{2}P\mathcal{D}_\varphi^{(2)}P^\top$ and U the matrix of associated eigenvectors. Since $\hat{\mathcal{D}}_\varphi$ serves as a reasonable estimate for \mathcal{D} , we apply classical multidimensional scaling of this estimated dissimilarity matrix to generate an estimated zero-skeleton mirror.

Definition 3.4 (Estimated zero-skeleton mirror). Let $\hat{\lambda}_1, \dots, \hat{\lambda}_c$ denote the c largest eigenvalues, in decreasing order, of $\hat{\mathcal{D}}_\varphi$. Put $\hat{S}_{ii} = \max\{\lambda_i, 0\}$. Let \hat{U} be the ordered matrix of eigenvectors associated to the c largest eigenvalues of $\hat{\mathcal{D}}_\varphi$. Let $\hat{\psi}(t_k)$ denote the k th row of $\hat{U}\hat{S}^{1/2}$. The estimated c -dimensional zero skeleton mirror is given by $\{\hat{\psi}(t_1), \dots, \hat{\psi}(t_m)\}$.

The following theorem from [\[2\]](#) allows us to control the error between the true and estimated zero-skeleton mirror.

Theorem 3.5 (Control between mirror and estimated mirror). Suppose \mathcal{D}_φ is approximately c Euclidean realizable. Let $\hat{U}, U \in \mathbb{R}^{m \times c}$ be the top c eigenvectors, and

$\hat{S}, S \in \mathbb{R}^{c \times c}$ be the diagonal matrices with diagonal entries equal to the top c eigenvalues of $-\frac{1}{2}P\hat{\mathcal{D}}_\varphi^{(2)}P^\top$ and $E_\varphi := -\frac{1}{2}P\mathcal{D}_\varphi^{(2)}P^\top$, respectively. Suppose $S_{i,i} > 0$ for $1 \leq i \leq c$. Then with overwhelming probability, there is a real orthogonal matrix $R \in \mathcal{O}^{c \times c}$ such that

$$\|\hat{U} - UR\|_F \leq \frac{2^{3/2}}{\lambda_c(E_\varphi)} \left(\frac{m \log(n)}{\sqrt{n}} + \left(\sum_{i=c+1}^m \lambda_i^2(E_\varphi) \right)^{1/2} \right).$$

Call this upper bound $B = B(n, m, c)$. The CMDS output satisfies

$$\|\hat{U}\hat{S}^{1/2} - US^{1/2}R\|_F \leq B\lambda_1^{1/2}(E_\varphi) \left(2 + 4B\kappa^{1/2} + (1 + 2B) \frac{m \log(n)}{\sqrt{n}\lambda_c(E_\varphi)} \right),$$

where $\kappa = \lambda_1(E_\varphi)/\lambda_c(E_\varphi)$. In particular, we have

$$\sum_{i=1}^m \|\hat{\psi}(t_i) - R\psi(t_i)\|^2 \leq B^2\lambda_1(E_\varphi) \left(2 + 4B\kappa^{1/2} + (1 + 2B) \frac{m \log(n)}{\sqrt{n}\lambda_c(E_\varphi)} \right)^2.$$

We can simplify the upper bound by further assuming that $c = 1$ and $\lambda_1(E_\varphi) \sim \Theta(m)$, this gives the following corollary.

Corollary 3.6. If additionally we require $c = 1$ and $\lambda_1(E_\varphi) \sim \Theta(m)$, then with overwhelming probability, there is a $r \in \{\pm 1\}$ and a constant C such that

$$\sum_{i=1}^m |\hat{\psi}(t_i) - r\psi(t_i)|^2 \leq \frac{C}{\lambda_1(E_\varphi)} \left(\frac{m \log(n)}{\sqrt{n}} + \sqrt{\sum_{i=2}^m \lambda_i^2(E_\varphi)} \right)^2.$$

In particular,

$$\max_{1 \leq i \leq m} |\hat{\psi}(t_i) - r\psi(t_i)| \leq C \left(\frac{m \log(n)}{\sqrt{n}\sqrt{\lambda_1(E_\varphi)}} + \sqrt{\frac{\sum_{i=2}^m \lambda_i^2(E_\varphi)}{\lambda_1(E_\varphi)}} \right).$$

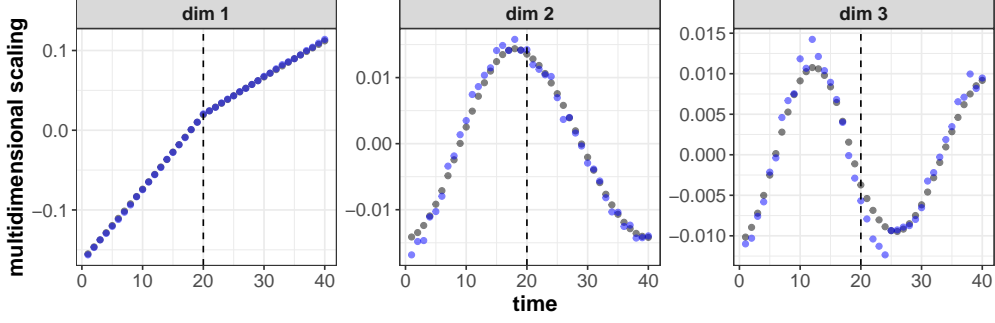


Figure 3.1. CMDS results on first 3 dimensions for *Model 2.20* with same setting as in *Figure 2.2*. The black dots are the numerical CMDS result on $\mathcal{D}_{\varphi_m}^{(2)}$. The blue dots are estimation from one realization of time series of graphs with $n = 1500$. Blue dots precisely aligns with the black dots in the first dimension. In the second dimension, the alignment of the estimated mirrors is less accurate, and the discrepancy increases further in the third dimension. For more details, see the final section of the supplement.

The results above guarantee that for a fixed number of graphs m in the TSG, as the number of vertices tends to infinity, at time t_i , the estimated mirror $\hat{\psi}(t_i)$ will be close to the true mirror $\psi(t_i)$ in the low dimensional Euclidean space. This is depicted in *Figure 3.1*, where, with $n = 1500$, the estimated mirror (blue dots) precisely aligns with the true mirror (black dots) in the first dimension. In the second dimension, the alignment of the estimated mirrors is less accurate, and the discrepancy increases further in the third dimension.

We exploit these results to show the consistency of localizing the changepoint using TSG realizations in the *Subsection 3.2*.

3.2. Consistency of the localizing estimator.

3.2.1. Consistency for exactly Euclidean 1-realizable latent position processes. In the following sections, we operate under the assumption that there is a single first-order changepoint, as outlined in *Model 2.25*, i.e., $p \neq q$. Our primary objective is to localize this changepoint as opposed to detecting whether there is a changepoint. We first consider a simpler case, where the LPP is exactly Euclidean 1-realizable with a piecewise linear mirror. Specifically, consider an exactly Euclidean 1-realizable latent position process with the mirror ψ defined by:

$$\psi(t) = \begin{cases} pt & \text{for } t < t^*, \\ qt + (p - q)t^* & \text{for } t \geq t^* \end{cases} \quad p \neq q.$$

This is equivalent to

$$\psi(t) = pt + (q - p)(t - t^*)I_{\{t > t^*\}} \quad t \in [0, T], t^* \in (0, T) \quad p \neq q.$$

This mirror is a continuous piecewise linear function with the slope change at t^* . Consider the time series of networks on n vertices at points $\mathcal{T} = \{t_1, \dots, t_m\}$ with this latent position process. Let $\{\hat{\psi}(t_i) | 1 \leq i \leq m\}$ denote the spectrally-derived estimated 0-skeleton mirror of [2]. Our goal is to localize t^* using $\hat{\psi}$. Throughout the section, without loss of generality, we will assume $t_1 = 0$ and $t_m = T$. That is the sampled time points will always include the endpoints.

To localize t^* we propose a simple localization estimator based on l_∞ regression and show its consistency. Without loss of generality, we can consider $p = 0$, $\Delta = q - p > 0$; that is:

$$\psi(t) = \Delta(t - t^*)I_{\{t > t^*\}} \quad t \in [0, T].$$

Let \mathcal{S} be the class of all continuous piecewise linear functions with exactly one changepoint t' on $(0, T)$:

$$\mathcal{S} = \{f | f(t) = \alpha + \beta_L(t - t') + (\beta_R - \beta_L)(t - t')I_{\{t > t'\}} \quad t \in [0, T]; \alpha, \beta_L, \beta_R \in \mathbb{R}, \beta_L \neq \beta_R\}.$$

Let $\mathcal{S}(\mathcal{T}) \subseteq \mathcal{S}$ be the subclass of continuous, piecewise linear functions on $[0, T]$ whose unique changepoint belongs to the set $\{t_1, \dots, t_m\}$:

$$\mathcal{S}(\mathcal{T}) = \{f | f(t) = \alpha + \beta_L(t - t') + (\beta_R - \beta_L)(t - t')I_{\{t > t'\}} \quad t \in [0, T]; t' \in \mathcal{T}, \alpha, \beta_L, \beta_R \in \mathbb{R}, \beta_L \neq \beta_R\}.$$

Let $\tilde{\psi}$ be the continuous, piecewise linear interpolation between the points $\{(t_i, \hat{\psi}(t_i)), t_i \in \mathcal{T}\}$. Consider the following minimization problem:

$$(3.2) \quad \min_{f \in \mathcal{S}(T)} \sup_{t \in [0, T]} |f - \tilde{\psi}(t)|.$$

We claim the following.

Lemma 3.7. *Consider two continuous piecewise linear functions f_1 and f_2 defined on $x \in [a, b]$, and each with a finite collection of changepoint sets denoted, respectively, by $\{t_1, t_2, \dots, t_m\} = \mathcal{T}_1$ and $\{t'_1, t'_2, \dots, t'_n\} = \mathcal{T}_2$. Suppose $\mathcal{T} = \mathcal{T}_1 \cup \mathcal{T}_2$. Then*

$$\sup_{x \in [a, b]} |f_1(x) - f_2(x)| = \max\{|f_1(a) - f_2(a)|, \max_{x \in \mathcal{T}} |f_1(x) - f_2(x)|, |f_1(b) - f_2(b)|\},$$

namely, the uniform norm of difference of two piecewise linear functions on an interval are determined only by their changepoints and endpoints of the interval.

Thus by Lemma 3.7 we find that (3.2) is equivalent to minimizing the problem below as $t_1 = 0$ and $t_m = T$:

$$\min_{f \in \mathcal{S}(\mathcal{T})} \max_{t \in \mathcal{T}} |f(t) - \hat{\psi}(t)|.$$

Let $h = h_{\hat{\psi}}$ be the minimizer in (3.2). Note that h is given by,

$$h = \arg \min_{f \in \mathcal{S}(\mathcal{T})} \max_{t \in \mathcal{T}} |f(t) - \hat{\psi}(t)|.$$

Generating h involves selecting an optimal time in \mathcal{T} as well as parameters of the piecewise linear function before and after the changepoint, to satisfy:

$$(3.3) \quad \hat{t}, \hat{\alpha}, \hat{\beta}_L, \hat{\beta}_R = \arg \min_{t' \in \mathcal{T}} \max_{\alpha, \beta_L, \beta_R, \beta_L \neq \beta_R} \left| \alpha + \beta_L(t - t') + (\beta_R - \beta_L)(t - t')I_{\{t > t'\}} - \hat{\psi}(t) \right|.$$

In practice if such \hat{t} is not unique, we will choose the earliest time that minimizes the objective function, that is:

$$(3.4) \quad \hat{t} = \min \left\{ t' : (t', \cdot) \in \arg \min_{\substack{t' \in \mathcal{T} \\ \alpha, \beta_L, \beta_R \\ \beta_L \neq \beta_R}} \max_{t \in \mathcal{T}} |\alpha + \beta_L(t - t') + (\beta_R - \beta_L)(t - t')I_{\{t > t'\}} - \hat{\psi}(t)| \right\}.$$

The quantity \hat{t} is our changepoint localization estimator, called the l_∞ localization estimator. To construct it, we consider every time point $t' \in \mathcal{T}$ and set each as a candidate changepoint; then we fit the given data to the best piecewise-linear function with knot at t' , seeking to minimize the l_∞ norm. We calculate the l_∞ loss $\ell(t')$ and choose the smallest candidate changepoint that minimizes $\ell(t')$. We summarize this procedure in [Algorithm 3.1](#). Note that \hat{t} is the same whether we use $\{\hat{\psi}(t_i) | 1 \leq i \leq m\}$ or $\{-\hat{\psi}(t_i) | 1 \leq i \leq m\}$.

Algorithm 3.1 l_∞ localization for piecewise linear data

- 1: Input: m pairs of observations $\{(t_1, y_1), (t_2, y_2), \dots, (t_m, y_m)\}$ with each $t_i \in \mathbb{R}, y_i \in \mathbb{R}$.
- 2: **for** k **from** 2 **to** $m - 1$:
- 3: Define

$$S_k := \min_{\alpha, \beta_L, \beta_R \in \mathbb{R}, \beta_L \neq \beta_R} \max_{1 \leq i \leq m} |\alpha + \beta_L(t_i - t_k) + (\beta_R - \beta_L)(t_i - t_k)I_{\{t_i > t_k\}} - y_i|.$$

- 4: Find the smallest k_0 such that $S_{k_0} = \min\{S_2, S_3, \dots, S_{m-1}\}$ and set $\hat{t} = t_{k_0}$.
 - 5: Output: \hat{t} .
-

We prove in the following lemma that we can upper bound the difference between \hat{t} and the true changepoint t^* .

Lemma 3.8. *Let $\psi(t) = at + b + \Delta(t - t^*)I_{\{t > t^*\}}$, $\Delta \neq 0$, and let $\tilde{\psi}$ be the continuous piecewise linear interpolation of $\{(t_i, \hat{\psi}(t_i)) | 1 \leq i \leq m\}$. Set*

$$\rho = \max_{1 \leq i \leq m-1} |t_i - t_{i+1}|.$$

Then the l_∞ changepoint localization estimator \hat{t} satisfies

$$|\hat{t} - t^*| \leq \left(\frac{4 \min_{w \in \{\pm 1\}} \sup_{t \in [0, T]} |\tilde{\psi}(t) - w\psi(t)|}{|\Delta|} + 2\rho \right) \frac{T}{\min\{T - t^*, t^*\}}.$$

The following theorem relies on the piecewise linearity of $\tilde{\psi}$ and [Corollary 3.6](#).

Theorem 3.9. *Consider an exactly Euclidean 1-realizable latent position process with α -Hölder mirror $\psi(t)$, where L denotes the Hölder constant on $t \in [0, T]$. Let $\{\hat{\psi}(t_i) | 1 \leq i \leq m\}$ denote the estimated mirror generated from the time series of graphs on n vertices with this LPP. Denote by $\tilde{\psi}(t)$ the piecewise linear interpolation between the points*

$\left\{ \left(t_i, \hat{\psi}(t_i) \right) \mid 1 \leq i \leq m \right\}$. Assume $t_1 = 0$, $t_m = T$, $\max_{1 \leq i \leq m} |t_i - t_{i+1}|^\alpha = \rho$ and $\lambda_1 \left(-\frac{1}{2} P \mathcal{D}^{(2)} P \right) \sim \Theta(m)$ where $\mathcal{D}^{(2)}$ is the $m \times m$ entrywise square of the distance matrix of the mirror $\psi(t)$, namely $\mathcal{D}_{ij}^{(2)} = \|\psi(t_i) - \psi(t_j)\|^2$ and $P = I - J/m$, where J is the $m \times m$ matrix with all entries equal to 1. Then there is a constant C and a $w_m \in \{\pm 1\}$ such that with high probability,

$$\sup_{t \in [0, T]} |\tilde{\psi}(t) - w_m \psi(t)| \leq \rho L + C \frac{m \log(n)}{\sqrt{n} \sqrt{\lambda_1 \left(-\frac{1}{2} P \mathcal{D}^{(2)} P \right)}}.$$

Combining these results, we obtain an upper bound on the error of the l_∞ localization estimator.

Theorem 3.10. Consider an exactly Euclidean 1-realizable latent position process with mirror $\psi(t) = at + b + \Delta(t - t^*)I_{\{t > t^*\}}$ $t \in [0, T]$, $\Delta \neq 0$, and $t^* \in (t_1, t_m)$. Let $\mathcal{T} = \{t_1, \dots, t_m\}$, where $t_1 = 0, t_m = T$, and define the centered version of $\psi_{\text{centered}}(t) = \psi(t) - \frac{1}{m} \sum_{i=1}^m \psi(t_i)$. Consider the time series of networks on n vertices at times in \mathcal{T} with this latent position process. Let \mathcal{D}_φ be the matrix of pairwise distances, which by 1-realizability satisfies $\mathcal{D}_{ij} = \|\psi(t_i) - \psi(t_j)\|$. Let $E_\varphi = -\frac{1}{2} P \mathcal{D}_\varphi^{(2)} P$, where $P = I - J/m$, for the $m \times m$ matrix of all ones, J . Assume that $\lambda_1(E_\varphi) \sim \Theta(m)$. Let $\{\hat{\psi}(t) \mid t \in \mathcal{T}\}$ denote the spectrally-derived estimated mirror of [2]. Let $\rho = \max_{1 \leq i < m} |t_i - t_{i+1}|$. Let \hat{t} be the l_∞ localization estimator in (3.3), namely:

$$\hat{t}, \hat{\alpha}, \hat{\beta}_L, \hat{\beta}_R = \arg \min_{\alpha, \beta_L, \beta_R, \beta_L \neq \beta_R} \max_{t' \in \mathcal{T}} |\alpha + \beta_L(t - t') + (\beta_R - \beta_L)(t - t')I_{\{t > t'\}} - \hat{\psi}(t)|.$$

Then there exists a constant C such that with high probability:

$$|\hat{t} - t^*| \leq \left(\frac{Cm \log(n)}{\sqrt{\sum_{i=1}^m \psi_{\text{centered}}^2(t_i)} |\Delta| \sqrt{n}} + 6\rho \right) \frac{T}{\min\{T - t^*, t^*\}}.$$

Corollary 3.11. When we uniformly sample the time points in $[0, T]$, that is, for any $1 \leq i < m$, $t_{i+1} - t_i = \frac{T}{m-1}$, then for large m and n , there exists a constant C such that with high probability:

$$|\hat{t} - t^*| \leq \left(\frac{C \log(n) \sqrt{mT}}{\sqrt{a^2 T^3 + \Delta^2 (T - t^*)^3} |\Delta| \sqrt{n}} + \frac{6T}{m-1} \right) \frac{T}{\min\{T - t^*, t^*\}}.$$

The upper bound demonstrates that the performance of \hat{t} is determined by the the change in slope of the mirror at the changepoint, as measured by $|\Delta|$; the number of time points m , which determines the fineness of the mesh; and the size of the graphs n , which determines the noise in the estimation of ψ . Note that this bound is also dependent on $\min\{t^*/T, (T - t^*)/T\}$, namely on how close the changepoint is to either of the endpoints of the interval.

A weakness of the given bound is the first term within the parentheses, which captures the noise in the estimation of $\psi(t)$ at a given time-point. To make this term shrink to zero,

we need n and m both to tend to infinity and $\frac{\log(n)\sqrt{m}}{\sqrt{n}} \rightarrow 0$, which requires n to tend to infinity faster than m . Since the sample size grows with the number of time points (m), one might suppose that even with a constant amount of variance in each estimate $\hat{\psi}(t)$ for $\psi(t)$, that is, with n fixed, as m grows, the error between the learned function (h) and the true one (ψ) should go to 0, which would cause this term to disappear. However, analysis of this term requires very delicate analysis of the output of CMDS under multiple sources of error: We have error arising from the finite number of time points m ; error from the finite number of vertices even if we knew the true latent position matrices, in the estimation of d_{MV} ; and error from the finite number of vertices because we have to estimate the latent position matrices from the observed adjacency matrices. As such, the errors between entries of the estimated and true distance matrices are correlated, and this can weaken the benefit of increasing m when there is a positive variance in each of the estimates $\hat{\psi}(t)$.

3.2.2. Consistency for in-fill summably asymptotically Euclidean 1-realizable model. In this section, we will generalize the above result for exactly Euclidean 1-realizable LPPs to the setting of in-fill summably asymptotically Euclidean 1-realizable LPPs where the asymptotic mirror is piecewise linear with a changepoint at t^* as in [Definition 2.24](#). We adapt [Theorem 3.9](#) for this case.

Theorem 3.12. *Assume an LPP is in-fill asymptotically 1-Euclidean realizable with the 0-skeleton mirror $\{\psi^{(m)}(t_i) | 1 \leq i \leq m\}$, and asymptotic mirror $\psi_0(t)$. Denote by $\tilde{\psi}_1^{(m)}(t)$ the piecewise linear interpolation between the points $\{(t_i, \psi_1^{(m)}(t_i)) | 1 \leq i \leq m\}$, as defined in [Definition 2.24](#). Put $E_{\psi^{(m)}} = -\frac{1}{2}P\mathcal{D}_{\psi^{(m)}}^{(2)}P$ where $\mathcal{D}_{\psi^{(m)}}^{(2)}$ is the $m \times m$ entry-wise square of the distance matrix of that mirror $\psi^{(m)}$, namely $(\mathcal{D}_{\psi^{(m)}}^{(2)})_{ij} = \|\psi^{(m)}(t_i) - \psi^{(m)}(t_j)\|^2$, and $P = I - J/m$, with J being the $m \times m$ all-ones matrix. Assume $t_1 = 0$, $t_m = T$ and $\lambda_1(E_{\psi^{(m)}}) \sim \Theta(m)$.*

Consider the first dimension of the estimated 0-skeleton mirror $\{\hat{\psi}_1^{(m)}(t_i) | 1 \leq i \leq m\}$ from the TSG generated by this LPP with n vertices. Denote by $\tilde{\hat{\psi}}_1^{(m)}(t)$ the piecewise linear interpolation between the points $\{(t_i, \hat{\psi}_1^{(m)}(t_i)) | 1 \leq i \leq m\}$.

Then, for n and m , sufficiently large, there exists a constant C and $w_m, w'_m \in \{\pm 1\}$ such that, with high probability:

$$\sup_{t \in [0, T]} |\tilde{\hat{\psi}}_1^{(m)}(t) - w'_m \psi_0(t)| \leq C \left(\frac{m \log(n)}{\sqrt{n} \sqrt{\lambda_1(E_{\psi^{(m)}})}} + \sqrt{\frac{\sum_{i=2}^m \lambda_i^2(E_{\psi^{(m)}})}{\lambda_1(E_{\psi^{(m)}})}} \right) + \sup_{t \in [0, T]} |\tilde{\hat{\psi}}_1^{(m)}(t) - w_m \psi_0(t)|.$$

Remark 3.13. Note that the mesh ρ , which originally appears in the upper bound of [Theorem 3.9](#), is implicitly involved in the term $\sup_{t \in [0, T]} |\tilde{\hat{\psi}}_1^{(m)}(t) - \psi_0(t)|$. In particular, when $|\tilde{\hat{\psi}}_1^{(m)}(t) - \psi_0(t)| \leq \alpha_n$ for each observed time $t \in \mathcal{T}$ and both functions are L -Lipschitz, the latter quantity may be bounded above by $\alpha_n + 2L\rho$. We require two different $w_m, w'_m \in \{\pm 1\}$ here to account for two sources of non-identifiability: one is the non-identifiability

between $\hat{\psi}_1^{(m)}$ and $\psi_1^{(m)}$, and the other is the non-identifiability between $\psi_1^{(m)}$ and ψ_0 . The second term in parentheses is the only one which is significantly different from the upper bound in [Theorem 3.9](#), and captures the distortion from approximating the asymptotically 1-d Euclidean realizable distance in \mathcal{D} with a 1-dimensional mirror.

This result leads to a similar upper bound for accuracy of the l_∞ localization estimator.

Theorem 3.14. *Consider an asymptotically Euclidean 1-realizable latent position process with zero-skeleton mirror $\{\psi^{(m)}(t_i), 1 \leq i \leq m\}$ and asymptotic mirror $\psi_0(t) = at + b + \Delta(t - t^*)I_{\{t > t^*\}}$, where $t \in [0, T]$ and $\Delta \neq 0$. Denote by $\tilde{\psi}_1^{(m)}$ the piecewise linear interpolation between the points*

$$\left\{ \left(t_i, \psi_1^{(m)}(t_i) \right) \mid 1 \leq i \leq m \right\} \subset \mathbb{R} \times \mathbb{R}.$$

Consider the time series of networks on n vertices at points $\mathcal{T} = \{t_1, \dots, t_m\}$ with this latent position process. Put $E_{\psi^{(m)}} = -\frac{1}{2}P\mathcal{D}_{\psi^{(m)}}^{(2)}P$, and $\mathcal{D}_{\psi^{(m)}}^{(2)}$ is the $m \times m$ entry-wise square of the distance matrix of the mirror $\psi^{(m)}$. Assume $t_1 = 0$, $t_m = T$, $t^ \in (t_1, t_m)$ and $\lambda_1(E_{\psi^{(m)}}) \sim \Theta(m)$. Let $\{\hat{\psi}_1^{(m)}(t_i) \mid 1 \leq i \leq m\}$ denote the spectrally-derived estimated first dimension mirror of [\[2\]](#). Let $\rho = \max_{1 \leq i < m} |t_i - t_{i+1}|$. Let \hat{t} be the l_∞ localization estimator in [\(3.3\)](#), namely:*

$$\hat{t}, \hat{\alpha}, \hat{\beta}_L, \hat{\beta}_R = \arg \min_{t' \in \mathcal{T}} \max_{\alpha, \beta_L, \beta_R, \beta_L \neq \beta_R} \left| \alpha + \beta_L(t - t') + (\beta_R - \beta_L)(t - t')I_{\{t > t'\}} - \hat{\psi}(t) \right|.$$

Then for m and n sufficiently large, there exists a constant C and a $w_m \in \{\pm 1\}$ such that with high probability:

$$|\hat{t} - t^*| \leq \left(\frac{Cm \log(n)}{\sqrt{n} \sqrt{\lambda_1(E_{\psi^{(m)}})} |\Delta|} + \frac{C \sqrt{\sum_{i=2}^m \lambda_i^2(E_{\psi^{(m)}})}}{\sqrt{\lambda_1(E_{\psi^{(m)}})} |\Delta|} + \frac{4 \sup_{t \in [0, T]} |\tilde{\psi}_1^{(m)}(t) - w_m \psi_0(t)|}{|\Delta|} + 2\rho \right) \frac{T}{\min\{T - t^*, t^*\}}.$$

Note by [Definition 2.24](#), if we further assume the LPP is in-fill summably asymptotically Euclidean 1-realizable, then as $m \rightarrow \infty$, $\lambda_1(E_{\psi^{(m)}}) \sim \Theta(m)$, $\sqrt{\frac{\sum_{i=2}^m \lambda_i^2(E_{\psi^{(m)}})}{\lambda_1(E_{\psi^{(m)}})}} \rightarrow 0$ and $\sup_{t \in [0, T]} |\tilde{\psi}_1^{(m)}(t) - w_m \psi_0(t)| \rightarrow 0$. Further if $\rho \rightarrow 0$ as $m \rightarrow \infty$ (for example, if $\rho = \frac{T}{m-1}$) and if $n \rightarrow \infty$ and $\frac{\log(n)\sqrt{m}}{\sqrt{n}} \rightarrow 0$, these conditions imply consistency of the estimator \hat{t} .

Corollary 3.15 (Consistency of \hat{t} for in-fill summably asymptotically 1-d Euclidean realizable with piecewise linear asymptotic mirror). *Consider a latent position process that is in-fill summably asymptotically 1-Euclidean realizable with asymptotic mirror $\psi_0(t) = at + b + \Delta(t - t^*)I_{\{t > t^*\}}$ $t \in [0, T]$. Consider the time series of networks on n vertices at points $\mathcal{T} = \{t_1, \dots, t_m\}$ with this latent position process. Assume $t_1 = 0$, $t_m = T$, and $t^* \in (t_1, t_m)$. Suppose that when $m \rightarrow \infty$, $\rho_m = \max_{1 \leq i \leq m-1} |t_i - t_{i+1}| \rightarrow 0$. Suppose also that when $n \rightarrow \infty$ and $m \rightarrow \infty$, $\frac{\log(n)\sqrt{m}}{\sqrt{n}} \rightarrow 0$. Then for the l_∞ estimator \hat{t} defined as above, we have with high probability that*

$$|\hat{t} - t^*| \rightarrow 0 \text{ as } m \rightarrow \infty, n \rightarrow \infty.$$

Note that [Model 2.25](#) satisfies the conditions in [Corollary 3.15](#). The only aspect we need to address is $t_1 = \frac{1}{m} \neq 0$. To address this, we can redefine the time points as follows: for $1 \leq i \leq m$, set $t_i = \frac{i-1}{m-1}$. Because the mirror focuses on interpoint distances and not specific time parameterizations, we obtain the following corollary for [Model 2.25](#).

Corollary 3.16. *Suppose n, m are such that $\frac{\log(n)\sqrt{m}}{\sqrt{n}} \rightarrow 0$ as $n, m \rightarrow \infty$. Using the l_∞ localization estimator on the observed time series of networks generated from [Model 2.25](#), we can consistently localize t^* as $n \rightarrow \infty$ and $m \rightarrow \infty$.*

3.3. Numerical experiments. As we have just shown, when an LPP is asymptotically Euclidean 1-realizable, for large n and m , the first dimension of the estimated mirror should yield consistent estimates for the changepoint t^* . In practice, however, there may still be useful signal contained in CMDS dimensions beyond the first as shown in [Figure 2.2](#). In the experiments of this section, we first compute the estimated mirror $\hat{\psi}$ in d dimensions, before considering the ISOMAP embedding of this curve into one dimension, denoted by $\hat{\psi}_{d \rightarrow 1}$. This embedding retains the piecewise linear structure, but incorporates additional signal from other dimensions. We write this iso-mirror via

$$(3.5) \quad \hat{\psi}_{d \rightarrow 1}(t) = \psi_Z(t) + \epsilon_t \quad t \in [0, 1],$$

where ψ_Z is defined for some $t^* \in (0, 1)$, $p, q > 0$, $p \neq q$ as

$$\psi_Z(t) = \begin{cases} pt & \text{for } t < t^* \\ qt + (p - q)t^* & \text{for } t \geq t^*. \end{cases}$$

Remark 3.17. We emphasize that two sources of error lie within the $\{\epsilon_t\}$: the first from finite network size n and the second from the finite number of sampled networks or time-points m . The first source of error, addressed in [\[2\]](#), arises because the draws from the LPP are random, as are the observed adjacency matrices A_t , making the estimated distances $\min_W \|\hat{X}_t - \hat{X}_s W\|/\sqrt{n}$ a noisy approximation of the true dissimilarity $d_{MV}(\varphi_m(t), \varphi_m(s))$. The second source of error is from the finite time-sampling of m networks. For finite m , the first dimension of the mirror of [Model 2.20](#) is not equal to ψ_Z , but instead converges to ψ_Z as $m \rightarrow \infty$. This error is deterministic and small for large m . Moreover, since we apply ISOMAP to an estimated mirror, these two sources of error in the mirror estimation propagate into the iso-mirror estimate $\hat{\psi}_{d \rightarrow 1}$ as well.

As before, we wish to localize t^* from an observed TSG whose latent positions follow a random walk LPP. We set the number of vertices, n , for the graphs and generate the time series of networks comprising m graphs according to [Model 2.25](#).¹ To prevent the graph from being too sparse, we choose the starting point as $c = 0.1$, resulting in $\delta = \frac{0.9}{m}$. Throughout, we set t^* to be $\frac{1}{2}$ and select an even number of time points m from the set 16, 24, 32, 40. We then choose $p = 0.4$ and $q = 0.3$.

For fixed values of n , m , $p = 0.4$, $q = 0.3$, and $t_m^* = \frac{m}{2}$, we generate a time series of graphs as follows. We fix a vector $X_{t_0} \in \mathbb{R}^{n \times 1}$, with all entries set to 0.1, representing the

¹All of our codes are available: <https://github.com/TianyiChen97/Euclidean-mirrors-and-first-order-changepoints-in-network-time-series>

Algorithm 3.2 Iso-mirror estimation

-
- 1: Input: TSG $\{A_1, A_2, \dots, A_m\}$, ASE dimension d_1 , CMDS dimension d .
 - 2: Compute $\hat{X}_t = \text{ASE}(A_t) \in \mathbb{R}^{n \times d_1}$, $1 \leq t \leq m$.
 - 3: Construct the distance matrix $\hat{\mathcal{D}} \in \mathbb{R}^{m \times m}$ where $\hat{\mathcal{D}}_{i,j} = \min_{W \in \mathcal{O}^{d_1 \times d_1}} \frac{1}{\sqrt{n}} \|\hat{\mathbf{X}}_t - \hat{\mathbf{X}}_s W\|_2$.
 - 4: Compute CMDS($\hat{\mathcal{D}}$) = $\{\hat{\psi}(1), \hat{\psi}(2), \dots, \hat{\psi}(m)\}$, with each $\hat{\psi}(t) \in \mathbb{R}^d$.
 - 5: Apply ISOMAP on $\{\hat{\psi}(1), \hat{\psi}(2), \dots, \hat{\psi}(m)\}$ using k nearest neighbors, where k is the smallest value such that the k -nearest-neighbor graph is connected, obtaining $\{\hat{\psi}_{d \rightarrow 1}(1), \hat{\psi}_{d \rightarrow 1}(2), \dots, \hat{\psi}_{d \rightarrow 1}(m)\}$, with each $\hat{\psi}_{d \rightarrow 1}(t) \in \mathbb{R}$.
 - 6: Output: $\{\hat{\psi}_{d \rightarrow 1}(1), \hat{\psi}_{d \rightarrow 1}(2), \dots, \hat{\psi}_{d \rightarrow 1}(m)\}$.
-

starting point for the n latent positions. For subsequent time points, we independently draw n samples $\{u_1, \dots, u_n\}$ from $\text{Bernoulli}(p)$. The i th entry of $(X_{t_k})_i = (X_{t_{k-1}})_i$ if $u_i = 0$, or $(X_{t_k})_i = (X_{t_{k-1}})_i + \frac{0.9}{m}$ if $u_i = 1$. This process repeats until $X_{\frac{m}{2}}$ is reached. For $X_{\frac{m}{2}+1}$, we switch the jump probability to $q = 0.3$. Eventually, we obtain $\{\hat{X}_{t_1}, \dots, X_{t_m}\}$ as the realized latent position matrices for n vertices. For each time, we generate an RDPG using the latent positions in X_t , obtaining a TSG $\{A_{t_1}, \dots, A_{t_m}\}$ as defined in [Definition 2.7](#).

For mirror estimation, we set the ASE embedding dimension to $d_1 = 1$, and consider various values of the CMDS embedding dimension d . We compute the covariance-based dissimilarity [\(3.1\)](#) between pairs of adjacency matrices A_{t_k}, A_{t_l} in $\{A_{t_1}, \dots, A_{t_m}\}$; then perform CMDS and output the iso-mirror estimate $\hat{\psi}_{d \rightarrow 1}$, as described in [Algorithm 3.2](#). We then compute the l_∞ localization estimator for the changepoint, following [Algorithm 3.1](#). In [Algorithm 3.1](#), the optimization at Step 3 is reformulated as a constrained linear programming problem, which we solve using the `lpSolveAPI`² function in R. This procedure is repeated for each Monte Carlo simulation, with each iteration yielding \hat{t}_{mc} .

To evaluate the performance of our estimator, we consider the squared error $(\hat{t}_{mc} - t^*)^2$ for each iteration. We run the Monte Carlo simulation $nmc = 2000$ times, and record the mean of these 2000 realizations as the mean square error (MSE):

$$\text{MSE} := \frac{1}{nmc} \sum_{mc=1}^{nmc} (\hat{t}_{mc} - t^*)^2.$$

Next, we calculate the sample standard deviation for the 2000 realizations:

$$\text{std} := \sqrt{\frac{1}{nmc - 1} \sum_{mc=1}^{nmc} \left((\hat{t}_{mc} - t^*)^2 - \text{MSE} \right)^2}.$$

Using a normal approximation, we can construct the confidence interval for the MSE as:

$$\text{CI} = \text{MSE} \pm \frac{1.96}{\sqrt{nmc}} \times \text{std},$$

and we plot the CI in [Figure 3.2](#) and [Figure 3.3](#).

²<https://cran.r-project.org/web/packages/lpSolveAPI/index.html>

In the first setting, we fix the CMDS embedding dimension $d = 1$ and choose $p = 0.4$, $q = 0.3$. Note when $d = 1$, applying ISOMAP to the CMDS mirror is unnecessary. We consider fixed $n = 800$ and vary m over 16, 24, 32, 40; next, we fix $m = 12$ and vary n over 200, 800, 1600. These results can be seen in Figure 3.2. For fixed m , MSE drops quickly with increasing n . For fixed $n = 800$, we also see that larger m is associated with significantly smaller MSE.

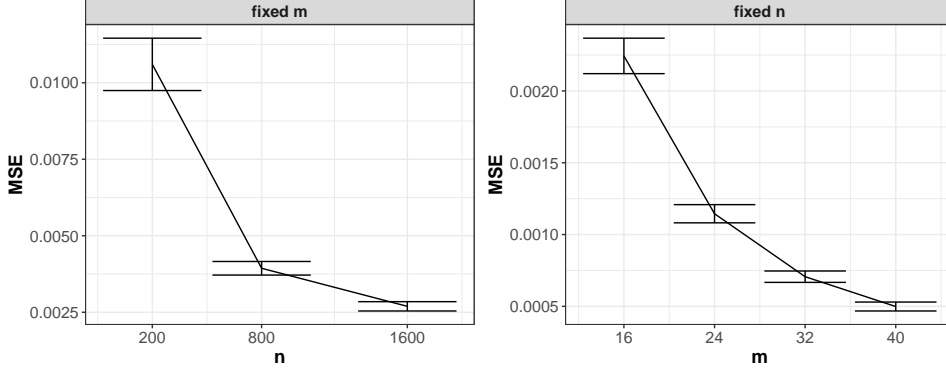


Figure 3.2. Accuracy of network changepoint estimator \hat{t} as a function of m and n when using the 1st dimension of the estimated mirror. $p = 0.4$, $q = 0.3$, $|p - q| = 0.1$, $nmc = 2000$ and $t^* = \frac{1}{2}$ fixed for both figures. Left: $m = 12$ fixed. Right: $n = 800$ fixed. We see the MSE tends to 0 for fixed $n = 800$ with m growing and for fixed $m = 12$ with n growing.

We examine how the accuracy of our localization estimator \hat{t} depends on the CMDS embedding dimension for the iso-mirror. In Figure 3.3 we see that as the embedding dimension increases, the MSE first decreases and then, eventually, increases. Recall in our model, higher dimensions still contain changepoint-relevant signal, so some number of additional dimensions can improve localization by reducing bias. However, embedding into significantly higher dimensions can also introduce additional variance, exhibited by the characteristic U shape of the MSE. Comparing the left two panels and the right two panels, we see as n increases, the variance drops dramatically, so increasing the dimension can improve estimation accuracy. Comparing the upper two panels and the lower two panels, we see the decreasing returns of increasing dimension: because of approximate one-dimensional Euclidean realizability, as m increases, there is less signal in the higher dimensions.

3.4. Analysis of brain organoid data. In this section, we apply our mirror-based techniques to real data, specifically a time series of brain organoid connectomes [23]. Brain organoids are self-organizing structures composed of roughly 2.5 million neural cells, generated from human induced pluripotent stem cells (hiPSCs) [16]. To characterize the functional development of the organoids, extracellular spontaneous electrical activity is recorded approximately weekly. Each time series consists of five minutes of recorded neural activity across 10 months. To approximate the functional connections between neurons, we apply the algorithm proposed in [23] and force the accepted degree of temporal approximation to be 0.

We obtain 38 functional connectivity networks on 181 vertices across 246 days. Since the

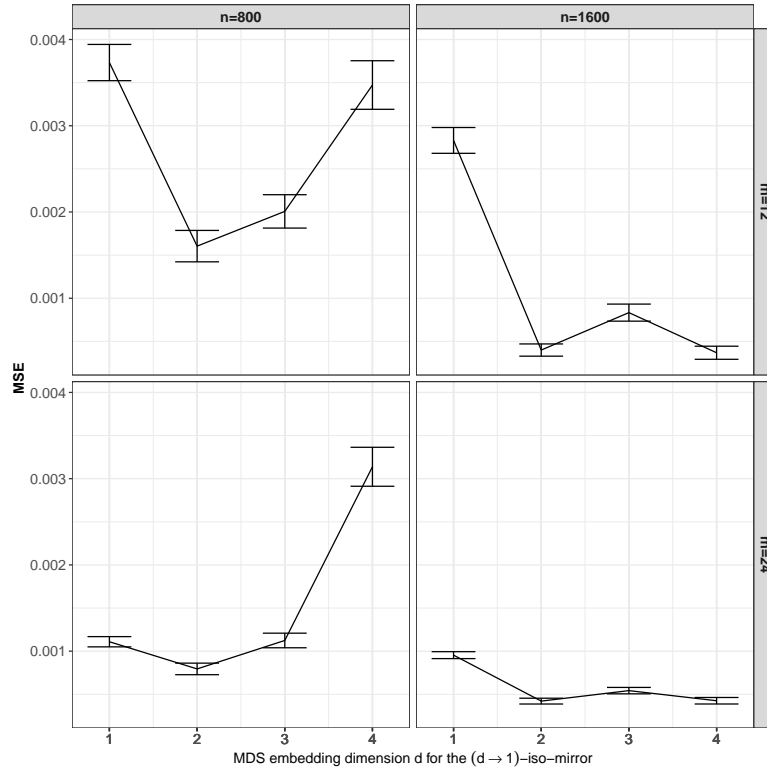


Figure 3.3. Accuracy of network changepoint estimator \hat{t} as a function of CMDS embedding dimension d when using the $(d \rightarrow 1)$ -iso-mirror $\hat{\psi}_{d \rightarrow 1}$. Upper left: $n = 800$, $m = 12$. Upper right: $n = 1600$, $m = 12$. Lower left: $n = 800$, $m = 24$. Lower right: $n = 1600$, $m = 24$. In all cases, $p = 0.4$, $q = 0.3$, $t^* = \frac{1}{2}$ and $nmc = 2000$. Comparing left two panels and right two panels, we see as n increases, the l_∞ estimator can yield improvement at higher embedding dimensions. Comparing the upper two panels and the lower two panels, we see the diminishing returns as to higher-dimensional embedding; as m increases, these higher dimensions contain less signal.

alignment of vertices among the networks is unknown, we apply the Fast Approximate Quadratic (FAQ) algorithm [30] to perform graph matching on all networks. We avoid the birth and death period, and choose only $m = 30$ graphs. We find the largest common connected component among the aligned networks, which contains $n = 44$ nodes, and we compute the estimated iso-mirror following Algorithm 3.2. Finally, we fit the data with l_∞ regression, specifying only 1 changepoint following Algorithm 3.1. This changepoint is estimated to occur on day 156 (see Figure 3.4). On the right panel, we also plot the control chart, which is simply the Frobenius norm difference between the adjacency matrices of two consecutive time points. Notably, this Frobenius norm difference consistently deviates from zero across almost all pairs of consecutive points. This pattern indicates that the time series of functional connectivity networks is in a state of constant flux. As a result, the zeroth-order changepoint Model 1.1, which would effectively classify every point as a changepoint, is not appropriate. Our proposed method, however, constructs a covariance-based dissimilarity matrix and applies CMDS and ISOMAP to obtain a one-dimensional Euclidean embedding, the iso-mirror,

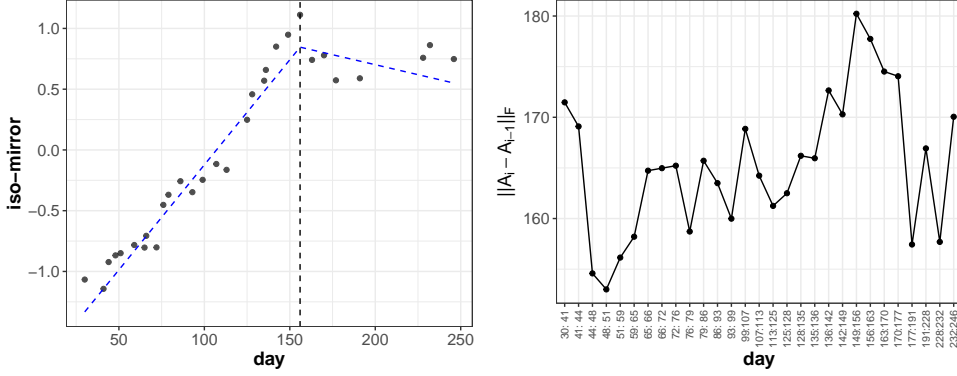


Figure 3.4. Real data example with time series of approximate functional connectivity graphs. On the left panel is iso-mirror result. The black dots are the estimated iso-mirror. The dashed blue piecewise linear curve is l_∞ regression fit, with the vertical line as the estimated changepoint at day 156. On the right panel is the control chart for pairwise Frobenius norm difference for the graphs. It also shows $\|A_{156} - A_{149}\|_F$ is the maximum. However the chart indicates the time series of networks are constantly changing and the underlying dynamic of the networks cannot be described as a zeroth-order changepoint [Model 1.1](#), which renders most changepoint algorithms based on such an assumption ineffective.

that takes into account all time stamps and the global dynamics of the time series of networks as opposed to considering consecutive pairwise differences. The piecewise linearity exhibited in the iso-mirror motivates the l_∞ estimator for changepoint localization.

4. Conclusion and Discussion. Changepoint localization for network time series is complicated by the fact that a changepoint can be more delicate than a simple shift in network distribution. For latent position process networks, we address three core points in this work: we formalize the concept of changepoints of different orders; we construct, in [Model 2.20](#), a time series of latent position networks with a first-order changepoint; and we show that such a changepoint can be successfully localized through spectral decompositions of network observations and spectrally-derived estimates of the associated Euclidean mirror. Building on work in [\[2\]](#), we also define asymptotic Euclidean realizability for a network time series, highlighting the significance of both network size n and the number of sampled time points m in such a time series.

The Euclidean mirror uses classical multidimensional scaling to represent a dissimilarity measure for latent position networks, and thus depends on the choice of embedding dimension and network dissimilarity. In our simulations, we underscore the efficacy of our mirror-based changepoint localization, with covariance dissimilarity, for [Model 2.20](#) and also illustrate the bias-variance trade-off associated to the embedding dimension. In our real data analysis of brain organoid networks, the mirror exhibits an approximately piecewise linear structure, and our algorithm locates a changepoint. Obtaining similarly powerful results for other kinds of data will require detailed analysis of different network dissimilarities and embedding dimensions.

There are multiple axes along which these results can be generalized and improved. In particular, finding a sharper bound in [Theorem 3.10](#) requires improved distributional results

on $\hat{\psi} - \psi$. Secondly, improved understanding of the effects of ISOMAP on the mirror estimate, particularly its impact on aggregating errors between the estimated and true mirror, will lead to improved understanding of the iso-mirror as a tool for network time series analysis.

The current paper is dedicated to the task of changepoint localization, but further exploration of the parameters in our estimated piecewise-linear mirror could lead to a test for both changepoint detection and localization. A related issue on this point is isolating and locating an indeterminate number of changepoints, which requires refined estimates beyond those we consider here. The success of mirror-based estimation for simple latent position networks and the associated provable guarantees for localization suggest that these techniques have wider promise in the analysis of evolving networks.

REFERENCES

- [1] J. AGTERBERG, Z. LUBBERTS, AND J. ARROYO, *Joint spectral clustering in multilayer degree-corrected stochastic blockmodels*, arXiv preprint arXiv:2212.05053, (2022).
- [2] A. ATHREYA, Z. LUBBERTS, Y. PARK, AND C. E. PRIEBE, *Discovering underlying dynamics in time series of networks*, arXiv preprint arXiv:2205.06877, (2022).
- [3] M. BHATTACHARJEE, M. BANERJEE, AND G. MICHAILIDIS, *Change point estimation in a dynamic stochastic block model*, Journal of machine learning research, 21 (2020), pp. 1–59.
- [4] G. E. BOX, G. M. JENKINS, G. C. REINSEL, AND G. M. LJUNG, *Time series analysis: forecasting and control*, John Wiley & Sons, 2015.
- [5] J. CAPE, M. TANG, AND C. E. PRIEBE, *The two-to-infinity norm and singular subspace geometry with applications to high-dimensional statistics*, Annual of Statistics, (2019).
- [6] T. CHEN, Y. PARK, A. SAAD-ELDIN, Z. LUBBERTS, A. ATHREYA, B. D. PEDIGO, J. T. VOGELSTEIN, F. PUPPO, G. A. SILVA, A. R. MUOTRI, ET AL., *Discovering a change point and piecewise linear structure in a time series of organoid networks via the iso-mirror*, Applied Network Science, 8 (2023), p. 45.
- [7] P. DIACONIS, S. GOEL, AND S. HOLMES, *Horseshoes in multidimensional scaling and local kernel methods*, The Annals of Applied Statistics, 2 (2008), pp. 777–807.
- [8] X. FAN, M. PENSKEY, F. YU, AND T. ZHANG, *Alma: Alternating minimization algorithm for clustering mixture multilayer network*, Journal of Machine Learning Research, 23 (2022), pp. 1–46.
- [9] R. HORN AND C. JOHNSON, *Matrix Analysis*, Cambridge University Press, 1985.
- [10] B.-Y. JING, T. LI, Z. LYU, AND D. XIA, *Community detection on mixture multilayer networks via regularized tensor decomposition*, The Annals of Statistics, 49 (2021), pp. 3181–3205.
- [11] A. JONES AND P. RUBIN-DELANCHY, *The multilayer random dot product graph*, arXiv preprint arXiv:2007.10455, (2020).
- [12] B. KEDEM AND K. FOKIANOS, *Regression models for time series analysis*, John Wiley & Sons, 2005.
- [13] Y. L. KEI, J. LI, H. LI, Y. CHEN, AND O. H. M. PADILLA, *Change point detection in dynamic graphs with generative model*, arXiv preprint arXiv:2404.04719, (2024).
- [14] K. Z. LIN AND J. LEI, *Dynamic clustering for heterophilic stochastic block models with time-varying node memberships*, arXiv preprint arXiv:2403.05654, (2024).
- [15] P. W. MACDONALD, E. LEVINA, AND J. ZHU, *Latent space models for multiplex networks with shared structure*, Biometrika, 109 (2022), pp. 683–706.
- [16] K. MUGURUMA, A. NISHIYAMA, H. KAWAKAMI, K. HASHIMOTO, AND Y. SASAI, *Self-organization of polarized cerebellar tissue in 3d culture of human pluripotent stem cells*, Cell reports, 10 (2015), pp. 537–550.
- [17] M. NOROOZI AND M. PENSKEY, *Sparse subspace clustering in diverse multiplex network model*, arXiv preprint arXiv:2206.07602, (2022).
- [18] O. H. M. PADILLA, Y. YU, AND C. E. PRIEBE, *Change point localization in dependent dynamic nonparametric random dot product graphs*, The Journal of Machine Learning Research, 23 (2022), pp. 10661–10719.

- [19] O. H. M. PADILLA, Y. YU, D. WANG, AND A. RINALDO, *Optimal nonparametric multivariate change point detection and localization*, IEEE Transactions on Information Theory, 68 (2021), pp. 1922–1944.
- [20] K. PANTAZIS, A. ATHREYA, J. ARROYO, W. N. FROST, E. S. HILL, AND V. LYZINSKI, *The importance of being correlated: Implications of dependence in joint spectral inference across multiple networks*, Journal of Machine Learning Research, 23 (2022), pp. 1–77.
- [21] S. PAUL AND Y. CHEN, *Spectral and matrix factorization methods for consistent community detection in multi-layer networks*, The Annals of Statistics, 48 (2020), pp. 230–250.
- [22] M. PENSKEY AND Y. WANG, *Clustering of diverse multiplex networks*, IEEE Transactions on Network Science and Engineering, (2024).
- [23] F. PUPPO, D. PRÉ, A. G. BANG, AND G. A. SILVA, *Super-selective reconstruction of causal and direct connectivity with application to in vitro ipsc neuronal networks*, Frontiers in Neuroscience, 15 (2021), p. 647877.
- [24] R. H. SHUMWAY, D. S. STOFFER, AND D. S. STOFFER, *Time series analysis and its applications*, vol. 3, Springer, 2000.
- [25] D. L. SUSSMAN, M. TANG, D. E. FISHKIND, AND C. E. PRIEBE, *A consistent adjacency spectral embedding for stochastic blockmodel graphs*, Journal of the American Statistical Association, 107 (2012), pp. 1119–1128.
- [26] M. TANG, D. L. SUSSMAN, AND C. E. PRIEBE, *Universally consistent vertex classification for latent position graphs*, Annals of Statistics, 41 (2013), pp. 1406 – 1430.
- [27] J. B. TENENBAUM, V. D. SILVA, AND J. C. LANGFORD, *A global geometric framework for nonlinear dimensionality reduction*, Science, 290 (2000), pp. 2319–2323.
- [28] M. W. TROSSET AND G. BUYUKBAS, *Rehabilitating isomap: euclidean representation of geodesic structure*, arXiv preprint arXiv:2006.10858, (2020).
- [29] N. VERZELEN, M. FROMONT, M. LERASLE, AND P. REYNAUD-BOURET, *Optimal change-point detection and localization*, The Annals of Statistics, 51 (2023), pp. 1586–1610.
- [30] J. T. VOGELSTEIN, J. M. CONROY, V. LYZINSKI, L. J. PODRAZIK, S. G. KRATZER, E. T. HARLEY, D. E. FISHKIND, R. J. VOGELSTEIN, AND C. E. PRIEBE, *Fast approximate quadratic programming for graph matching*, PLoS One, 10 (2015), p. e0121002, <http://dx.doi.org/10.1371/journal.pone.0121002>.
- [31] D. WANG, Y. YU, AND A. RINALDO, *Optimal change point detection and localization in sparse dynamic networks*, arXiv e-prints, (2021).
- [32] F. WANG, W. LI, O. H. M. PADILLA, Y. YU, AND A. RINALDO, *Multilayer random dot product graphs: Estimation and online change point detection*, arXiv preprint arXiv:2306.15286, (2023).
- [33] P. J. WOLFE AND S. C. OLHEDE, *Nonparametric graphon estimation*. arXiv preprint arXiv: 1309.5936, 2013.
- [34] M. ZHU AND A. GHODSI, *Automatic dimensionality selection from the scree plot via the use of profile likelihood*, Computational Statistics & Data Analysis, 51 (2006), pp. 918–930.
- [35] T. ZUZUL, E. C. PAHNKE, J. LARSON, P. BOURKE, N. CAURVINA, N. P. SHAH, F. AMINI, J. WESTON, Y. PARK, J. VOGELSTEIN, ET AL., *Dynamic silos: Increased modularity in intra-organizational communication networks during the covid-19 pandemic*, arXiv preprint arXiv:2104.00641, (2021).

Appendix A. Proof of Lemma 2.19.

Proof. Suppose $t, t' \in \{1, 2, \dots, n\}$ and $t' < t$. Put $a := t - t'$. Since X_t is a one-dimensional random variable,

$$\begin{aligned} d_{MV}(X_t, X_{t'})^2 &= \min_{W \in \mathcal{O}^{1 \times 1}} \left\| \mathbb{E}[(X_t - WX_{t'})(X_t - WX_{t'})^\top] \right\|_2 \\ &= \min_W |\mathbb{E}[X_t^2 - 2WX_tX_{t'} + W^2X_{t'}^2]|. \end{aligned}$$

To address the minimization over orthogonal matrices, observe that in one dimension, orthogonal transformations correspond only to multiplication by 1 or -1 . So we need only consider the two cases $W = 1$ or $W = -1$. Since $X_t \geq 0$ for all t , $\mathbb{E}[X_tX_{t'}] \geq 0$. Thus $W = 1$

minimizes the above, and we conclude that

$$d_{MV}(X_t, X_{t'})^2 = \mathbb{E}[(X_t - X_{t'})^2].$$

The increment $X_t - X_{t'}$ satisfies $X_t - X_{t'} = V_a \delta$, where V_a is a Binomial random variable with a trials and success probability p , namely $V_a \sim \text{Binomial}(a, p)$. Thus

$$\begin{aligned} \mathbb{E}[(X_t - X_{t'})^2] &= \delta^2 \mathbb{E}[V_a^2] \\ &= (a^2 p^2 + a(p - p^2)) \delta^2. \end{aligned}$$

Appendix B. Proof of Lemma 2.23.

Proof. First we consider [Model 2.18](#). Fix $\beta \in [0, 1]$. Put $t_{\beta, m} = \lfloor m\beta \rfloor$. Then $X_{t_{\beta, m}}^{(m)} = \frac{V_{t_{\beta, m}, p}}{m}$, where $V_{t_{\beta, m}}$ is a Binomial random variable with $t_{\beta, m}$ trials and success probability p . Therefore, $\mathbb{E}[X_{t_{\beta, m}}^{(m)}] = \frac{\lfloor m\beta \rfloor p}{m}$ and as $m \rightarrow \infty$,

$$\mathbb{E}[X_{t_{\beta, m}}^{(m)} - \beta p]^2 = \mathbb{E}[X_{t_{\beta, m}}^{(m)} - \mathbb{E}[X_{t_{\beta, m}}^{(m)}] + \mathbb{E}[X_{t_{\beta, m}}^{(m)}] - \beta p]^2 = \frac{\lfloor m\beta \rfloor p(1-p)}{m^2} + \left(\frac{\lfloor m\beta \rfloor p}{m} - \beta p \right)^2 \rightarrow 0.$$

Thus $X_{t_{\beta, m}}^{(m)} \xrightarrow{L^2} \beta p = Z_\beta$.

Now consider [Model 2.20](#). Again fix $t^*, \beta \in [0, 1]$ and put $t_{\beta, m} = \lfloor m\beta \rfloor$ and $t_m^* = \lfloor mt^* \rfloor$. If $\beta \leq t^*$, then $t_{\beta, m} = \lfloor m\beta \rfloor \leq \lfloor t^* m \rfloor = t_m^*$; thus $\tilde{X}_{t_{\beta, m}}^{(m)} = X_{t_{\beta, m}}^{(m)}$ and the result follows from what we have proved above.

When $\beta > t^*$, note for any $x \in \mathbb{R}$, $\lfloor x \rfloor - 1 < x \leq \lfloor x \rfloor$, and thus $\lfloor m\beta \rfloor - \lfloor t^* m \rfloor > m\beta - (mt^* + 1)$. Then for all $m > \frac{1}{\beta - t^*}$, $t_{\beta, m} > t_m^*$. In this case, $\tilde{X}_{t_{\beta, m}}^{(m)} = \frac{V_{t_m^*, p} + V_{t_{\beta, m} - t_m^*, q}}{m}$. Therefore $\mathbb{E}[\tilde{X}_{t_{\beta, m}}^{(m)}] = \frac{\lfloor mt^* \rfloor p + (\lfloor m\beta \rfloor - \lfloor mt^* \rfloor)q}{m}$ and as $m \rightarrow \infty$,

$$\mathbb{E}[\tilde{X}_{t_{\beta, m}}^{(m)} - (t^* p + \beta q - t^* q)]^2 = \mathbb{E} \left[\left[\frac{V_{t_m^*, p}}{m} - t^* p \right] + \left[\frac{V_{t_{\beta, m} - t_m^*, q}}{m} - (\beta q - t^* q) \right] \right]^2.$$

Both squared terms $\mathbb{E} \left[\frac{V_{t_m^*, p}}{m} - t^* p \right]^2$ and $\mathbb{E} \left[\frac{V_{t_{\beta, m} - t_m^*, q}}{m} - (\beta q - t^* q) \right]^2$ converge to zero by the same argument as before. For the cross term, namely $\mathbb{E} \left[\frac{V_{t_m^*, p}}{m} - t^* p \right] \left[\frac{V_{t_{\beta, m} - t_m^*, q}}{m} - (\beta q - t^* q) \right]$, note that $V_{t_m^*, p}$ is independent of $V_{t_{\beta, m} - t_m^*, q}$, so the expectation of the product is equal to the product of the expectation, with converging to zero.

Appendix C. Proof of Lemma 2.22.

Proof. When $\varphi(t)$ is deterministic, for any x, y :

$$\begin{aligned} d_{MV}(\varphi(x), \varphi(y))^2 &= \min_{W \in \mathcal{O}^{d \times d}} \left\| \mathbb{E}[(\varphi(x) - W\varphi(y))(\varphi(x) - W\varphi(y))^\top] \right\|_2^2 \\ &= \min_{W \in \mathcal{O}^{d \times d}} \left\| (\varphi(x) - W\varphi(y))(\varphi(x) - W\varphi(y))^\top \right\|_2^2 \\ &= \min_{W \in \mathcal{O}^{d \times d}} \|\varphi(x) - W\varphi(y)\|_2^2 \\ &= (\|\varphi(x)\|_2 - \|\varphi(y)\|_2)^2. \end{aligned}$$

The last equality follows since $\|\varphi(x) - W\varphi(y)\|_2^2 \geq (\|\varphi(x)\|_2 - \|\varphi(y)\|_2)^2$ always holds and there exists a W such that $\varphi(x)$ and $\varphi(y)$ are linearly dependent, in which case the lower bound is achieved. The result now follows after centering the mirror. \blacksquare

Appendix D. Proof of Theorem 2.26.

Proof. We first state certain properties of the two distance matrices \mathcal{D}_{φ_m} and \mathcal{D}_Z . Denote the eigenvalues and the corresponding orthonormal eigenvectors of $-\frac{1}{2}P\mathcal{D}_Z^{(2)}P$ and $-\frac{1}{2}P\mathcal{D}_{\varphi_m}^{(2)}P$ respectively by $\lambda_1, \lambda_2, \dots, \lambda_m$ and U_1, U_2, \dots, U_m ; $\tilde{\lambda}_1, \tilde{\lambda}_2, \dots, \tilde{\lambda}_m$ and $\tilde{U}_1, \tilde{U}_2, \dots, \tilde{U}_m$. Then the k th dimension of the mirror for Model 2.25 is: $\sqrt{\tilde{\lambda}_k}\tilde{U}_k$. Since \mathcal{D}_Z is exactly Euclidean 1-realizable, by Theorem 2.15, its mirror is $\sqrt{\lambda_1}U_1$.

Property D.1. $\lambda_1 \sim \Theta(m)$, $\lambda_i = 0$ for $i \geq 2$. And $\|U_1\|_{2 \rightarrow \infty} \sim O\left(\frac{1}{\sqrt{m}}\right)$.

Proof. Since \mathcal{D}_Z is exactly 1-d Euclidean realizable with mirror $\sqrt{\lambda_1}U_1$, $-\frac{1}{2}P\mathcal{D}_Z^{(2)}P = \lambda_1 U_1 U_1^\top$ where $\sqrt{\lambda_1}U_1 = (\psi_Z(\frac{1}{m}), \psi_Z(\frac{2}{m}), \dots, \psi_Z(\frac{m}{m}))^\top$. Thus, since ψ_Z^2 is Riemann integrable,

$$\frac{\lambda_1}{m} = \frac{\sum_{i=1}^m \psi_Z^2(\frac{i}{m})}{m} \rightarrow \int_0^1 \psi_Z^2(x) dx = C \text{ as } m \rightarrow \infty.$$

That is, $\lambda_1 \sim \Theta(m)$. Next, since

$$\left\| \sqrt{\lambda_1}U_1 \right\|_{2 \rightarrow \infty} = \left\| \left(\psi_Z\left(\frac{1}{m}\right), \psi_Z\left(\frac{2}{m}\right), \dots, \psi_Z\left(\frac{m}{m}\right) \right)^\top \right\|_{2 \rightarrow \infty} \leq \max_{t \in [0,1]} |\psi_Z(t)| \leq p + q + c_0,$$

thus $\|U_1\|_{2 \rightarrow \infty} \sim O\left(\frac{1}{\sqrt{m}}\right)$. \blacksquare

Property D.2. $\|\mathcal{D}_{\varphi_m}^{(2)} - \mathcal{D}_Z^{(2)}\|_\infty \sim O(1)$, and $\tilde{\lambda}_1 \sim \Theta(m)$, $\tilde{\lambda}_i \sim O(1)$ for $i \geq 2$.

Proof. Because $(\mathcal{D}_{\varphi_m}^{(2)} - \mathcal{D}_Z^{(2)})_{i,j} \sim O\left(\frac{1}{m}\right)$ for all i, j , we get $\|\mathcal{D}_{\varphi_m}^{(2)} - \mathcal{D}_Z^{(2)}\|_\infty \sim O(1)$ and $\|\mathcal{D}_{\varphi_m}^{(2)} - \mathcal{D}_Z^{(2)}\|_F \sim O(1)$. Also note $\|P\|_2 = 1$, so

$$\left\| \frac{1}{2}P(\mathcal{D}_{\varphi_m}^{(2)} - \mathcal{D}_Z^{(2)})P \right\|_F^2 \leq \left\| \frac{1}{2}(\mathcal{D}_{\varphi_m}^{(2)} - \mathcal{D}_Z^{(2)}) \right\|_F^2 \|P\|_2^4 = \left\| \frac{1}{2}(\mathcal{D}_{\varphi_m}^{(2)} - \mathcal{D}_Z^{(2)}) \right\|_F^2 \sim O(1).$$

Thus

$$\left\| \frac{1}{2}P(\mathcal{D}_{\varphi_m}^{(2)} - \mathcal{D}_Z^{(2)})P \right\|_2^2 \leq \left\| \frac{1}{2}P(\mathcal{D}_{\varphi_m}^{(2)} - \mathcal{D}_Z^{(2)})P \right\|_F^2 \sim O(1).$$

Weyl's theorem guarantees that $|\lambda_k - \tilde{\lambda}_k| \leq \left\| \frac{1}{2}P(\mathcal{D}_{\varphi_m}^{(2)} - \mathcal{D}_Z^{(2)})P \right\|_2$ for all k . Since $\lambda_1 \sim \Theta(m)$ and $\lambda_i = 0$ for $i \geq 2$, the result follows. \blacksquare

Property D.3. There exists a $w = 1$ or $w = -1$ such that: $\|\sqrt{\tilde{\lambda}_1}\tilde{U}_1 - w\sqrt{\lambda_1}U_1\|_{2 \rightarrow \infty} \rightarrow 0$ as $m \rightarrow \infty$.

Proof. From [Property D.1](#), we know $\lambda_1 \sim \Theta(m)$ and $\|U_1\|_{2 \rightarrow \infty} \sim O(\frac{1}{\sqrt{m}})$. There exists a $w = 1$ or $w = -1$ such that:

$$\begin{aligned} & \left\| \sqrt{\tilde{\lambda}_1} \tilde{U}_1 - w \sqrt{\lambda_1} U_1 \right\|_{2 \rightarrow \infty} \leq \sqrt{\tilde{\lambda}_1} \left\| \tilde{U}_1 - w U_1 \right\|_{2 \rightarrow \infty} + \left| \sqrt{\tilde{\lambda}_1} - \sqrt{\lambda_1} \right| \|U_1\|_{2 \rightarrow \infty} \\ & \leq \sqrt{\tilde{\lambda}_1} c \frac{\left\| \frac{1}{2} P(\mathcal{D}_{\varphi_m}^{(2)} - \mathcal{D}_Z^{(2)}) P \right\|_{\infty}}{\lambda_1} \|U_1\|_{2 \rightarrow \infty} + \left| \sqrt{\tilde{\lambda}_1} - \sqrt{\lambda_1} \right| \|U_1\|_{2 \rightarrow \infty} \\ & \leq \left(\frac{c \sqrt{\tilde{\lambda}_1} \left\| \frac{1}{2} P(\mathcal{D}_{\varphi_m}^{(2)} - \mathcal{D}_Z^{(2)}) P \right\|_{\infty}}{\lambda_1} + \left| \sqrt{\tilde{\lambda}_1} - \sqrt{\lambda_1} \right| \right) \|U_1\|_{2 \rightarrow \infty}. \end{aligned}$$

The second inequality uses Theorem 4.2 in [\[5\]](#), which we quote here:

Theorem D.4. *Let $X, E \in \mathbb{R}^{p \times p}$ be symmetric matrices where $\text{rank}(X) = r$ and X has spectral decomposition $X = U \Lambda U^T$ and $X + E = \hat{U} \hat{\Lambda} \hat{U}^T + \hat{U}_{\perp} \hat{\Lambda}_{\perp} \hat{U}_{\perp}^T$. Suppose the leading eigenvalues of X are given by $|\lambda_1| \geq |\lambda_2| \geq \dots \geq |\lambda_r| \geq 0$. If $|\lambda_r| \geq 4\|E\|_{\infty}$, then there exists an orthogonal matrix $W_U \in O_r$ such that*

$$\left\| \hat{U} - U W_U \right\|_{2 \rightarrow \infty} \leq 14 \left(\frac{\|E\|_{\infty}}{|\lambda_r|} \right) \|U\|_{2 \rightarrow \infty}.$$

The condition that $|\lambda_1| > 4 \left\| P(\mathcal{D}_{\varphi_m}^{(2)} - \mathcal{D}_Z^{(2)}) P \right\|_{\infty}$ is satisfied since $\lambda_1 \sim \Theta(m)$ and

$$\left\| P(\mathcal{D}_{\varphi_m}^{(2)} - \mathcal{D}_Z^{(2)}) P \right\|_{\infty} \leq \left\| \mathcal{D}_{\varphi_m}^{(2)} - \mathcal{D}_Z^{(2)} \right\|_{\infty} \|P\|_{\infty}^2 \leq 4 \left\| \mathcal{D}_{\varphi_m}^{(2)} - \mathcal{D}_Z^{(2)} \right\|_{\infty} \sim O(1).$$

Now we consider $\left| \sqrt{\tilde{\lambda}_1} - \sqrt{\lambda_1} \right|$. Note that

$$\left| \sqrt{\tilde{\lambda}_1} - \sqrt{\lambda_1} \right| = \frac{|\tilde{\lambda}_1 - \lambda_1|}{\sqrt{\tilde{\lambda}_1} + \sqrt{\lambda_1}} \sim \frac{O(1)}{\Theta(\sqrt{m})} \sim O\left(\frac{1}{\sqrt{m}}\right).$$

Thus for large m , there exists a constant C such that $\left| \sqrt{\tilde{\lambda}_1} - \sqrt{\lambda_1} \right| \leq \frac{C}{\sqrt{m}}$, and the above term can be further bounded by

$$\left(\frac{c \left(\sqrt{\lambda_1} + \frac{C}{\sqrt{m}} \right) \left\| \frac{1}{2} P(\mathcal{D}_{\varphi_m}^{(2)} - \mathcal{D}_Z^{(2)}) P \right\|_{\infty}}{\lambda_1} + \left| \sqrt{\tilde{\lambda}_1} - \sqrt{\lambda_1} \right| \right) \|U_1\|_{2 \rightarrow \infty} \sim O\left(\frac{1}{m}\right)$$

as required. ■

Property D.5. $\frac{\sum_{i=2}^m \tilde{\lambda}_i^2}{\lambda_1} \rightarrow 0$ as $m \rightarrow \infty$.

Proof. By the Hoffman-Wielandt inequality [\[9\]](#), we derive

$$\sum_{i=2}^m (\tilde{\lambda}_i - \lambda_i)^2 \leq \left\| \frac{1}{2} P(\mathcal{D}_Z^{(2)} - \mathcal{D}_{\varphi_m}^{(2)}) P \right\|_F^2 \sim O(1).$$

Note $\lambda_i = 0$ for $i \geq 2$. Thus we have

$$\sum_{i=2}^m \tilde{\lambda}_i^2 \sim O(1).$$

Recall from [Property D.2](#) that $\tilde{\lambda}_1 \sim \Theta(m)$; then $\frac{\sum_{i=2}^m \tilde{\lambda}_i^2}{\tilde{\lambda}_1} \sim O\left(\frac{1}{m}\right)$ and the result follows. \blacksquare

Now we prove each of the claims in [Theorem 2.26](#). Note that Claim (2) is immediate because

$$\max_{i,j \in \{1,2,\dots,m\}} \left| \left(\mathcal{D}_{\varphi_m}^{(2)} - \mathcal{D}_Z^{(2)} \right)_{i,j} \right| \leq \frac{1}{4m}$$

for any m . Claims (3) and (4) are proved in [Property D.2](#) and [Property D.5](#).

For Claim (1), recall $\tilde{\psi}_1^{(m)}$ is the piecewise linear interpolation between the points

$$\left\{ \left(t_i, \left(\sqrt{\tilde{\lambda}_1} \tilde{U}_1 \right)_i \right), 1 \leq i \leq m \right\},$$

Consider the unique extension of this function to a function that is linear on interval $[0, t_2]$; through this extension, we define $\tilde{\psi}_1^{(m)}$ on $[0, t_1]$ on as well. Denote by $\tilde{\psi}_Z$ the piecewise linear interpolation between the points $\left\{ \left(t_i, \left(\sqrt{\tilde{\lambda}_1} \tilde{U}_1 \right)_i \right), 1 \leq i \leq m \right\} = \left\{ \left(t_i, \psi_Z \left(\frac{i}{m} \right) \right), 1 \leq i \leq m \right\}$. Then

$$\sup_{t \in [0,1]} \left| \tilde{\psi}_1^{(m)}(t) - \psi_Z(t) \right| \leq \sup_{t \in [0,1]} \left| \tilde{\psi}_1^{(m)}(t) - \tilde{\psi}_Z(t) \right| + \sup_{t \in [0,1]} \left| \tilde{\psi}_Z(t) - \psi_Z(t) \right|.$$

Observe that $\tilde{\psi}_1^{(m)}(t)$ and $\tilde{\psi}_Z$ are both piecewise linear interpolations at the same time points $\{t_1, t_2, \dots, t_m\}$, where $t_m = 1$. By linearity on $[0, t_2]$, we have

$$\left| \tilde{\psi}_1^{(m)}(0) - \tilde{\psi}_Z(0) \right| \leq 3 \max_{t \in \{t_1, t_2\}} \left| \tilde{\psi}_1^{(m)}(t) - \tilde{\psi}_Z(t) \right|.$$

Now because of [Lemma 3.7](#) and [Property D.3](#), we see that

$$\sup_{t \in [0,1]} \left| \tilde{\psi}_1^{(m)}(t) - \tilde{\psi}_Z(t) \right| = \max_{t \in \{0, t_1, t_2, \dots, t_m\}} \left| \tilde{\psi}_1^{(m)}(t) - \tilde{\psi}_Z(t) \right| \leq 3 \left\| \sqrt{\tilde{\lambda}_1} \tilde{U}_1 - \sqrt{\lambda_1} U_1 \right\|_{2 \rightarrow \infty} \rightarrow 0.$$

Consider $\sup_{t \in [0,1]} \left| \tilde{\psi}_Z(t) - \psi_Z(t) \right|$. Recall that $\tilde{\psi}_Z(t) = \psi_Z(t)$ for $t \in \{t_1, t_2, \dots, t_m\}$ and both of them are piecewise linear.

Then $\sup_{t \in [0,1]} \left| \tilde{\psi}_Z(t) - \psi_Z(t) \right| > 0$ only if $t^* \notin \{t_1, t_2, \dots, t_m\}$. When $t^* \notin \{t_1, t_2, \dots, t_m\}$, $\tilde{\psi}_Z$ and ψ_Z disagree only on the interval $[t_i, t_{i+1}]$ that contains t^* . We can bound the difference by

$$\sup_{t \in [0,1]} \left| \tilde{\psi}_Z(t) - \psi_Z(t) \right| = \left| \frac{(p-q)(t_{i+1} - t^*)(t^* - t_i)}{t_{i+1} - t_i} \right| \leq |p-q| |t_{i+1} - t_i| = \frac{|p-q|}{m},$$

because $t_i = \frac{i}{m}$ for all $i \in \{1, \dots, m\}$. Thus this term also tends to 0 as $m \rightarrow \infty$, as required.

Appendix E. Proof of Corollary 3.6.

Proof. We first find an upper bound for B : note that

$$\min_{R \in \mathcal{O}^{c \times c}} \|\hat{U} - UR\|_F \leq \|\hat{U} - U\|_F \leq \|\hat{U}\|_F + \|U\|_F \leq 2\sqrt{c}$$

because \hat{U} and U both have c orthonormal columns. Thus $B \leq \sqrt{2c}$. Since $c = 1$, $B \leq \sqrt{2}$ and $\kappa = 1$. Additionally, we have $\lambda_1(E_\varphi) \sim \Theta(m)$, and since $\frac{\log(n)}{\sqrt{n}} \leq 8$ for $n \in \mathbb{N}^+$, we get

$$\begin{aligned} \sum_{i=1}^m \|\hat{\psi}(t_i) - R\psi(t_i)\|^2 &\leq B^2 \lambda_1(E_\varphi) \left(2 + 4B\kappa^{1/2} + (1 + 2B) \frac{m \log(n)}{\sqrt{n} \lambda_1(E_\varphi)} \right)^2 \\ &\leq B^2 \lambda_1(E_\varphi) \left(2 + 4\sqrt{2} + (1 + 2\sqrt{2}) 8 \right) \\ &\leq CB^2 \lambda_1(E_\varphi). \end{aligned}$$

Then plug $B = \frac{2^{3/2}}{\lambda_1(E_\varphi)} \left(\frac{m \log(n)}{\sqrt{n}} + \left(\sum_{i=c+1}^m \lambda_i^2(E_\varphi) \right)^{1/2} \right)$ back we get the result. \blacksquare

Appendix F. Proof of Lemma 3.7.

Proof. Order the set \mathcal{T} as $\mathcal{T} = \{x_1, x_2, \dots, x_k\}$, and $x_i \leq x_{i+1}$ for all $1 \leq i \leq k-1$. Note $k \leq m+n$. Then on any $[x_i, x_{i+1}]$, f_1 and f_2 both are linear functions; hence the function $f_1(x) - f_2(x)$ is also a linear function on $[x_i, x_{i+1}]$. Further, the function $|f_1(x) - f_2(x)|$ is convex on the compact and convex set $[x_i, x_{i+1}]$. Thus its maximum is obtained at some extreme point of the set $[x_i, x_{i+1}]$; these extreme points are $\{x_i, x_{i+1}\}$. We have that

$$\sup_{x \in [x_i, x_{i+1}]} |f_1(x) - f_2(x)| = \max\{|f_1(x_i) - f_2(x_i)|, |f_1(x_{i+1}) - f_2(x_{i+1})|\}.$$

This also holds on $[a, x_1]$ and $[x_k, b]$. Partiting the interval $[a, b]$ as $[a, b] = [a, x_1] \cup [x_1, x_2] \cdots \cup [x_k, b]$, we derive

$$\begin{aligned} &\sup_{x \in [a, b]} |f_1(x) - f_2(x)| \\ &= \max\left\{ \sup_{t \in [a, x_1]} |f_1(t) - f_2(t)|, \sup_{t \in [x_1, x_2]} |f_1(t) - f_2(t)|, \dots, \sup_{t \in [x_k, b]} |f_1(t) - f_2(t)| \right\} \\ &= \max\{|f_1(a) - f_2(a)|, \max_{x \in \mathcal{T}} |f_1(x) - f_2(x)|, |f_1(b) - f_2(b)|\}. \end{aligned} \quad \blacksquare$$

Appendix G. Proof of Lemma 3.8.

Proof. Without loss of generality, assume $0 < \hat{t} < t^*$. Next, because $h \in \mathcal{S}(\{\hat{t}\})$, we have:

$$\min_{f \in \mathcal{S}(\{\hat{t}\})} \sup_{t \in [0, T]} |f(t) - \psi(t)| \leq \sup_{t \in [0, T]} |h(t) - \psi(t)|.$$

The minimization on the left hand side may be written as:

$$\begin{aligned} &\min_{f \in \mathcal{S}(\{\hat{t}\})} \sup_{t \in [0, T]} |f(t) - \psi(t)| \\ &= \min_{\alpha, \beta_L, \beta_R, \beta_L \neq \beta_R} \sup_{t \in [0, T]} |\alpha + \beta_L(t - \hat{t}) + (\beta_R - \beta_L)(t - \hat{t})I_{\{t > \hat{t}\}} - at - b - \Delta(t - t^*)I_{\{t > t^*\}}| \\ &= \min_{\alpha, \beta_L, \beta_R, \beta_L \neq \beta_R} \sup_{t \in [0, T]} |\alpha' + \beta'_L(t - \hat{t}) + (\beta'_R - \beta'_L)(t - \hat{t})I_{\{t > \hat{t}\}} - |\Delta|(t - t^*)I_{\{t > t^*\}}|, \end{aligned}$$

where we have defined $\alpha' = \text{sgn}(\Delta)(\alpha - b)$, $\beta'_L = \text{sgn}(\Delta)(\beta_L - a)$, $\beta'_R = \text{sgn}(\Delta)(\beta_R - a)$. Applying Lemma 3.7, we see that this is equivalent to

$$\begin{aligned} & \min_{f \in \mathcal{S}(\{\hat{t}\})} \sup_{t \in [0, T]} |f(t) - \psi(t)| \\ &= \min_{\alpha', \beta'_L, \beta'_R, \beta'_L \neq \beta'_R} \max\{|\alpha'|, |\alpha' - \beta'_L \hat{t}|, |\alpha' + \beta'_R(t^* - \hat{t})|, |\alpha' + \beta'_R(T - \hat{t}) - |\Delta|(T - t^*)|\}. \end{aligned}$$

By checking the Karush-Kuhn-Tucker (KKT) conditions (see H), we find that the minimum is given by

$$\frac{T - t^*}{2(T - \hat{t})} |\hat{t} - t^*| |\Delta|$$

from which we conclude that

$$\frac{T - t^*}{2(T - \hat{t})} |\hat{t} - t^*| |\Delta| \leq \sup_{t \in [0, T]} |h(t) - \psi(t)|.$$

To bound the right hand side, we introduce $\psi^T(t)$ as a translation of $\psi(t)$ such that the changepoint is at the sampled time t_{k^*} that is closest to t^* , the changepoint of the true $\psi(t)$. That is:

$$\psi^T(t) = at + b + \Delta(t - t_{k^*})I_{\{t > t_{k^*}\}}.$$

Note $\psi^T(t) \in \mathcal{S}(\mathcal{T})$ and recall $\max_{t \in \mathcal{T}} |h - \hat{\psi}(t)| = \min_{f \in \mathcal{S}(\mathcal{T})} \max_{t \in \mathcal{T}} |f - \hat{\psi}(t)|$. From this, we find that

$$\max_{t \in \mathcal{T}} |h(t) - \hat{\psi}(t)| \leq \max_{t \in \mathcal{T}} |\psi^T(t) - \hat{\psi}(t)|.$$

We also have $\sup_{t \in [0, T]} |\psi^T(t) - \psi(t)| = |\Delta| |t^* - t_{k^*}| \leq |\Delta| \rho$.

Because $h(t) - \hat{\psi}(t)$ and $\psi^T(t) - \hat{\psi}(t)$ are both continuous piecewise linear functions with changepoints in \mathcal{T} , again Lemma 3.7 implies that

$$\max_{t \in \mathcal{T}} |h(t) - \hat{\psi}(t)| = \sup_{t \in [0, T]} |h(t) - \tilde{\psi}(t)|, \quad \max_{t \in \mathcal{T}} |\psi^T(t) - \hat{\psi}(t)| = \sup_{t \in [0, T]} |\psi^T(t) - \tilde{\psi}(t)|.$$

Therefore,

$$(G.1) \quad \sup_{t \in [0, T]} |h(t) - \tilde{\psi}(t)| \leq \sup_{t \in [0, T]} |\psi^T(t) - \tilde{\psi}(t)|.$$

Next, note that

$$\begin{aligned}
 \frac{T-t^*}{2(T-\hat{t})}|\hat{t}-t^*||\Delta| &\leq \sup_{t \in [0,T]} |h(t) - \psi(t)| \\
 &\leq \sup_{t \in [0,T]} |h(t) - \tilde{\psi}(t)| + \sup_{t \in [0,T]} |\tilde{\psi}(t) - \psi(t)| \\
 &\leq \sup_{t \in [0,T]} |\psi^T(t) - \tilde{\psi}(t)| + \sup_{t \in [0,T]} |\tilde{\psi}(t) - \psi(t)| \text{ by (G.1)} \\
 &\leq \sup_{t \in [0,T]} |\psi^T(t) - \psi(t)| + \sup_{t \in [0,T]} |\psi(t) - \tilde{\psi}(t)| + \sup_{t \in [0,T]} |\tilde{\psi}(t) - \psi(t)| \\
 &= \sup_{t \in [0,T]} |\psi^T(t) - \psi(t)| + 2 \sup_{t \in [0,T]} |\tilde{\psi}(t) - \psi(t)| \\
 &\leq |\Delta|\rho + 2 \sup_{t \in [0,T]} |\tilde{\psi}(t) - \psi(t)|.
 \end{aligned}$$

Dividing both sides by $\frac{T-t^*}{2(T-\hat{t})}|\Delta|$ and recalling that

$$\frac{T-\hat{t}}{T-t^*} \leq \frac{T}{\min\{t^*, T-t^*\}},$$

we conclude that

$$|\hat{t}-t^*| \leq \left(\frac{4 \sup_{t \in [0,T]} |\tilde{\psi}(t) - \psi(t)|}{|\Delta|} + 2\rho \right) \frac{T}{\min\{T-t^*, t^*\}}.$$

For any given $\{\hat{\psi}(t_i) | 1 \leq i \leq m\}$ we can also use $\{-\hat{\psi}(t_i) | 1 \leq i \leq m\}$ to get \hat{t} which is equivalent to using $\{\hat{\psi}(t_i) | 1 \leq i \leq m\}$. This yields

$$|\hat{t}-t^*| \leq \left(\frac{4 \sup_{t \in [0,T]} |-\tilde{\psi}(t) - \psi(t)|}{|\Delta|} + 2\rho \right) \frac{T}{\min\{T-t^*, t^*\}}.$$

Combining the previous two results, we conclude that

$$|\hat{t}-t^*| \leq \left(\frac{4 \min_{w \in \{\pm 1\}} \sup_{t \in [0,T]} |\tilde{\psi}(t) - w\psi(t)|}{|\Delta|} + 2\rho \right) \frac{T}{\min\{T-t^*, t^*\}}.$$

Appendix H. Verification of KKT condition.

First we recall the Karush-Kuhn-Tucker (KKT) conditions for the minimizer of the constrained optimization problem, stated below:

Theorem H.1 (Necessary conditions for the minimizer). *Consider the constrained optimization problem:*

$$\begin{aligned}
 &\min f(\mathbf{x}) \\
 &\text{subject to } g_1(\mathbf{x}) \leq 0, \dots, g_k(\mathbf{x}) \leq 0
 \end{aligned}$$

Suppose the minimizer of this problem is \mathbf{x}^* . If $g_{i_1}(\mathbf{x}^*) = g_{i_2}(\mathbf{x}^*) = \dots = g_{i_j}(\mathbf{x}^*) = 0$ (namely, the constraints are active), and $g_l(\mathbf{x}^*) < 0$ for $l \notin \{i_1, \dots, i_j\}$, then if the gradients of the active constraints evaluated at \mathbf{x}^* are linearly independent, there exist $\lambda_1, \dots, \lambda_j \geq 0$ such that:

$$(H.1) \quad -\nabla f(\mathbf{x}^*) = \sum_{s=1}^j \lambda_s \nabla g_{i_s}(\mathbf{x}^*).$$

Our optimization problem of interest is given by:

$$\min_{\alpha', \beta'_L, \beta'_R, \beta'_L \neq \beta'_R} \max\{|\alpha'|, |\alpha' - \beta'_L \hat{t}|, |\alpha' + \beta'_R(t^* - \hat{t})|, |\alpha' + \beta'_R(T - \hat{t}) - |\Delta|(T - t^*)|\}.$$

Therefore, without loss of generality, we may take $\Delta > 0$, and our optimization problem can be written as:

$$\min_{\alpha, \beta_L, \beta_R, \beta_L \neq \beta_R} \max\{|\alpha|, |\alpha - \beta_L \hat{t}|, |\alpha + \beta_R(t^* - \hat{t})|, |\alpha + \beta_R(T - \hat{t}) - \Delta(T - t^*)|\}.$$

This is equivalent to:

$$\begin{aligned} \min \quad & f(z, \alpha, \beta_L, \beta_R) = z; \\ \text{subject to} \quad & g_1 = \alpha - z \leq 0, \\ & g_2 = -\alpha - z \leq 0, \\ & g_3 = \alpha - \beta_L \hat{t} - z \leq 0, \\ & g_4 = -\alpha + \beta_L \hat{t} - z \leq 0, \\ & g_5 = -\alpha - \beta_R(t^* - \hat{t}) - z \leq 0, \\ & g_6 = \alpha + \beta_R(t^* - \hat{t}) - z \leq 0, \\ & g_7 = -\alpha - \beta_R(T - \hat{t}) + \Delta(T - t^*) - z \leq 0, \\ & g_8 = \alpha + \beta_R(T - \hat{t}) - \Delta(T - t^*) - z \leq 0. \end{aligned}$$

We recall $\Delta > 0, 0 < \hat{t} < t^* < T$. Then

$$\nabla f(z, \alpha, \beta_L, \beta_R) = (1, 0, 0, 0)^\top.$$

Because $\nabla f(z, \alpha, \beta_L, \beta_R)$ never vanishes, the minimizer \mathbf{x}^* must be on the boundary of the feasible set, so at least one of the constraints is active: namely, there exists i with $g_i(\mathbf{x}^*) = 0$. In the following analysis, we enumerate all possible sets of active constraints and find the only feasible ones, which yields the minimizer.

For ease of notation, we form a matrix ∇ with its i th column to be $\nabla g_i(z, \alpha, \beta_L, \beta_R)$:

$$\nabla = \begin{bmatrix} -1 & -1 & -1 & -1 & -1 & -1 & -1 & -1 \\ 1 & -1 & -1 & 1 & -1 & 1 & -1 & 1 \\ 0 & 0 & \hat{t} & -\hat{t} & 0 & 0 & 0 & 0 \\ 0 & 0 & 0 & 0 & -(t^* - \hat{t}) & t^* - \hat{t} & -(T - \hat{t}) & T - \hat{t} \end{bmatrix}.$$

Also if only one of the constraints are active at the minimizer, then by KKT conditions H.1, there exists a $\lambda \geq 0$ such that:

$$\lambda \nabla g_i = (-1, 0, 0, 0)^\top.$$

This equation has no solution for any $i \in \{1, 2, \dots, 8\}$. Thus at least two of constraints are active at the minimizer. In addition, we note if any one of the four pairs of $(g_1, g_2), (g_3, g_4), (g_5, g_6), (g_7, g_8)$ are active, then $z = 0$, then $\Delta = 0$, which violates our assumption. Thus in none of these four pairs can both constraints be active.

For g_3 and g_4 , because $\hat{t} > 0$ and only g_3 and g_4 have the third entry non-zero, to satisfy the equation H.1, the coefficients of ∇g_3 and ∇g_4 have to be equal. Since at most one of these coefficients is nonzero, they must both be zero.

Now we consider the case in which the active constraints are among g_5, g_6, g_7, g_8 . Suppose the only constraints that are active are (g_5, g_7) . (Note that it is possible that g_3 or g_4 is also active, but we have shown the corresponding coefficient is zero, and hence this cannot influence the equation H.1.) In this case, the equation H.1 has no solution. Similarly, (g_6, g_8) cannot be the only active constraints. Note that this still holds if one of g_1, g_2 is active. Then for (g_5, g_8) to satisfy the equation H.1, we find $T = t^*$ which again violates our assumption. A similar analysis holds for (g_6, g_7) . The above analysis shows that one of g_1 and g_2 has to be active, that is $z = \alpha$ or $z = -\alpha$.

Now if (g_2, g_5, g_8) are all active, then we have:

$$z = -\alpha = -\alpha - \beta_R(t^* - \hat{t}) = \alpha + \beta_R(T - \hat{t}) - \Delta(T - t^*)$$

Thus $\beta_R = 0$ and $z = \frac{\Delta(t^* - T)}{2} < 0$, and this is infeasible.

For (g_1, g_5, g_8) we have:

$$z = \alpha = -\alpha - \beta_R(t^* - \hat{t}) = \alpha + \beta_R(T - \hat{t}) - \Delta(T - t^*)$$

Thus $\alpha = -\frac{\Delta(t^* - \hat{t})(T - t^*)}{2(T - \hat{t})}$, $z = -\frac{\Delta(t^* - \hat{t})(T - t^*)}{2(T - \hat{t})} < 0$, which is infeasible.

For (g_1, g_6, g_7) , by solving the active constraints similarly we have $z = \alpha = \frac{\Delta(T - t^*)}{2}$, which is feasible. Then we check the KKT condition H.1:

$$\begin{cases} -\lambda_1 - \lambda_6 - \lambda_7 = -1 \\ \lambda_1 + \lambda_6 - \lambda_7 = 0 \\ (t^* - \hat{t}) \lambda_6 - (T - \hat{t}) \lambda_7 = 0 \end{cases}$$

Solving this, we note $\lambda_1 = \frac{1}{2} \left(1 - \frac{T - \hat{t}}{t^* - \hat{t}}\right) < 0$, which violates the KKT conditions.

For (g_2, g_6, g_7) we have:

$$z = -\alpha = \alpha + \beta_R(t^* - \hat{t}) = -\alpha - \beta_R(T - \hat{t}) + \Delta(T - t^*)$$

Thus $\alpha = -\frac{\Delta(t^* - \hat{t})(T - t^*)}{2(T - \hat{t})}$, $z = \frac{\Delta(t^* - \hat{t})(T - t^*)}{2(T - \hat{t})}$. We next check KKT conditions by solving the equations:

$$\begin{cases} -\lambda_2 - \lambda_6 - \lambda_7 = -1 \\ -\lambda_2 + \lambda_6 - \lambda_7 = 0 \\ (t^* - \hat{t}) \lambda_6 - (T - \hat{t}) \lambda_7 = 0 \end{cases}$$

We obtain the following solutions:

$$\begin{cases} \lambda_2 = \frac{1}{2} \left(1 - \frac{t^* - \hat{t}}{T - \hat{t}} \right) > 0 \\ \lambda_6 = \frac{1}{2} > 0 \\ \lambda_7 = \frac{t^* - \hat{t}}{2(T - \hat{t})} > 0 \end{cases}$$

This satisfies the KKT condition, and the corresponding gradients are linearly independent:

$$\begin{bmatrix} -1 & -1 & -1 \\ -1 & 1 & -1 \\ 0 & 0 & 0 \\ 0 & t^* - \hat{t} & -(T - \hat{t}) \end{bmatrix}$$

Because these active constraints at the minimizer are the only set that satisfies the KKT conditions (with the possible addition of g_3 or g_4), these active constraints yield that $z = \frac{\Delta(t^* - \hat{t})(T - t^*)}{2(T - \hat{t})}$. We conclude the minimum value of this optimization problem is $\frac{\Delta(t^* - \hat{t})(T - t^*)}{2(T - \hat{t})}$.

Appendix I. Proof of Theorem 3.9. First we state a useful lemma.

Lemma I.1. *Assume that $\psi(t)$ is an α -Hölder continuous with constant L function on $t \in [0, T]$. Let the sampled times $\{t_1, t_2, \dots, t_m\} \subset [0, T]$ be given and assume $t_1 = 0$ and $t_m = T$. Denote*

$$\max_{1 \leq i < m} |t_i - t_{i+1}|^\alpha = \rho.$$

If $\tilde{\psi}(t)$ is the piecewise linear interpolation between the points $\{(t_i, \psi(t_i)), 1 \leq i \leq m\}$, then

$$\sup_{t \in [0, T]} |\tilde{\psi}(t) - \psi(t)| \leq \rho L.$$

Proof. For $t \in [0, T]$ and $t \neq t_k$ for $1 \leq k \leq m$, because we assume $t_1 = 0$ and $t_m = T$, we can always find t_i and t_{i+1} where $1 \leq i < m$ such that $t \in (t_i, t_{i+1})$. Then there exists a $0 < \lambda < 1$ such that $t = \lambda t_i + (1 - \lambda)t_{i+1}$. Since $\tilde{\psi}(t)$ is the piecewise linear interpolation between the points $\{(t_i, \psi(t_i)), 1 \leq i \leq m\}$, it follows that

$$\tilde{\psi}(t) = \lambda \psi(t_i) + (1 - \lambda) \psi(t_{i+1}).$$

We thus have

$$\begin{aligned} |\tilde{\psi}(t) - \psi(t)| &= |\lambda(\psi(t_i) - \psi(t)) + (1 - \lambda)(\psi(t_{i+1}) - \psi(t))| \\ &\leq \lambda L |t - t_i|^\alpha + (1 - \lambda) L |t_{i+1} - t|^\alpha \\ &\leq (\lambda L + (1 - \lambda)L) |t_{i+1} - t_i|^\alpha \\ &= L |t_i - t_{i+1}|^\alpha. \end{aligned}$$

■

Thus

$$\sup_{t \in [0, T]} |\tilde{\psi}(t) - \psi(t)| \leq L \max_{1 \leq i \leq m} |t_i - t_{i+1}|^\alpha = \rho L.$$

Now we are ready to prove Theorem 3.9. We know there exists a $w_m \in \{\pm 1\}$ such that

$$\begin{aligned} \sup_{t \in [0, T]} |\tilde{\psi}(t) - w_m \psi(t)| &\leq \sup_{t \in [0, T]} |\tilde{\psi}(t) - w_m \tilde{\psi}(t)| + \sup_{t \in [0, T]} |w_m \tilde{\psi}(t) - w_m \psi(t)|, \\ &\leq \max_{1 \leq i \leq m} |\hat{\psi}(t_i) - w_m \psi(t_i)| + \rho L, \quad \text{by Lemma 3.7 and Lemma I.1} \\ &\leq \frac{Cm \log(n)}{\sqrt{n} \sqrt{\lambda_1(-\frac{1}{2} P \mathcal{D}^{(2)} P)}} + \rho L, \quad \text{by Corollary 3.6 and exactly 1-realizability.} \end{aligned}$$

so the result follows.

Appendix J. Proof of Theorem 3.10.

Proof. The true mirror ψ has the form $\psi(t) = at + b + \Delta(t - t^*)I_{\{t > t^*\}}$ for $t \in [0, T]$, so $\psi(t)$ is Lipschitz continuous with constant $|\Delta|$. Note that for any $w_m \in \{\pm 1\}$,

$$\min_{w \in \{\pm 1\}} \sup_{t \in [0, T]} |\tilde{\psi}(t) - w\psi(t)| \leq \sup_{t \in [0, T]} |\tilde{\psi}(t) - w_m \psi(t)|.$$

The result now follows from Theorem 3.9 and Lemma 3.8.

Let $\psi(t) = at + b + \Delta(t - t^*)I_{\{t > t^*\}}$ for $t \in [0, T]$. Define $\mathcal{D}^{(2)}$ to be the matrix whose i, j th entry is $\mathcal{D}_{ij}^{(2)} = |\psi(t_i) - \psi(t_j)|^2$ for t_i and t_j belonging to $\{t_1, \dots, t_m\}$. Put $c = \frac{1}{m} \sum_{i=1}^m \psi(t_i)$ and $\psi_{centered}(t) = \psi(t) - c$. Denote by Ψ_m the $m \times 1$ vector

$$\Psi_m = (\psi_{centered}(t_1), \psi_{centered}(t_2), \dots, \psi_{centered}(t_m)).$$

Note that $-\frac{1}{2} P \mathcal{D}^{(2)} P = \Psi_m \Psi_m^\top$, and hence

$$\lambda_1 \left(-\frac{1}{2} P \mathcal{D}^{(2)} P \right) = \lambda_1 \left(\Psi_m \Psi_m^\top \right) = \Psi_m^\top \Psi_m = \sum_{i=1}^m \psi_{centered}^2(t_i)$$

as required. ■

Appendix K. Proof of Corollary 3.11.

Proof. In this case $\rho = \frac{T}{m-1}$ and $t_i = \frac{(i-1)T}{m-1}$ for $1 \leq i \leq m$. Set $c_m = \frac{1}{m} \sum_{i=1}^m \psi(t_i)$. By the Riemann integrability of $\psi(t)$, $c_m \rightarrow \frac{1}{T} \int_0^T \psi(t) dt$ as $m \rightarrow \infty$. Thus, we observe that

$$\begin{aligned} \frac{1}{m} \sum_{i=1}^m \psi_{centered}^2(t_i) &= \frac{1}{m} \sum_{i=1}^m (\psi(t_i) - c_m)^2 \\ &= \frac{1}{m} \sum_{i=1}^m (\psi(t_i)^2 - 2\psi(t_i)c_m + c_m^2) \\ &= \left\{ \frac{m-1}{mT} \sum_{i=1}^m \frac{T}{m-1} \psi^2 \left(\frac{(i-1)T}{m-1} \right) \right\} - c_m^2 \\ &\rightarrow \frac{1}{T} \int_0^T \psi^2(t) dt - \left(\frac{1}{T} \int_0^T \psi(t) dt \right)^2. \end{aligned}$$

Since $\psi(t) = at + b + \Delta(t - t^*)I_{\{t > t^*\}}$, these integrals can be computed explicitly. The value of the integral is clearly independent of b , so without loss of generality we set $b = 0$. Then we obtain

$$\begin{aligned} \int_0^T \psi(t) dt &= a \frac{T^2}{2} + \Delta \frac{(T - t^*)^2}{2}, \\ \int_0^T \psi^2(t) dt &= a^2 \frac{T^3}{3} + a\Delta(T - t^*)^2 \frac{2T + t^*}{3} + \Delta^2 \frac{(T - t^*)^3}{3}. \end{aligned}$$

So the limit equals

$$\begin{aligned} \frac{1}{T} \int_0^T \psi^2(t) dt - \left(\frac{1}{T} \int_0^T \psi(t) dt \right)^2 &= a^2 \frac{T^2}{12} + a\Delta \frac{(T - t^*)^2}{2T} \left(\frac{T + 2t^*}{3} \right) + \Delta^2 \frac{(T - t^*)^3}{3T^2} \left(\frac{T + 3t^*}{4} \right) \\ &\geq \frac{1}{12T} (a^2 T^3 + \Delta^2 (T - t^*)^3). \end{aligned} \quad \blacksquare$$

Appendix L. Proof of Theorem 3.12.

Proof. We begin by bounding this quantity as:

$$\sup_{t \in [0, T]} \left| \tilde{\psi}_1^{(m)}(t) - w'_m \psi_0(t) \right| \leq \sup_{t \in [0, T]} \left| \tilde{\psi}_1^{(m)}(t) - w_m \tilde{\psi}_1^{(m)}(t) \right| + \sup_{t \in [0, T]} \left| w_m \tilde{\psi}_1^{(m)}(t) - w'_m \psi_0(t) \right|.$$

We need to consider $w_m \in \{\pm 1\}$ and $w'_m \in \{\pm 1\}$ here to account for the nonidentifiability between $\hat{\psi}_1^{(m)}$ and $\psi_1^{(m)}$ and the nonidentifiability between $\psi_1^{(m)}$ and ψ_0 . To bound the first term, we apply Lemma 3.7 to get

$$\sup_{t \in [0, T]} \left| \tilde{\psi}_1^{(m)}(t) - w_m \tilde{\psi}_1^{(m)}(t) \right| \leq \max_{1 \leq i \leq m} \left| \hat{\psi}_1^{(m)}(t_i) - w_m \psi_1^{(m)}(t_i) \right|$$

From Corollary 3.6, we know there exists a $w_m \in \{\pm 1\}$ and a constant C such that with high probability,

$$\max_{1 \leq i \leq m} \left| \hat{\psi}_1^{(m)}(t_i) - w_m \psi_1^{(m)}(t_i) \right| \leq C \left(\frac{m \log(n)}{\sqrt{n} \sqrt{\lambda_1 \left(-\frac{1}{2} P \mathcal{D}^{(2)} P \right)}} + \sqrt{\frac{\sum_{i=2}^m \lambda_i^2 \left(-\frac{1}{2} P \mathcal{D}^{(2)} P \right)}{\lambda_1 \left(-\frac{1}{2} P \mathcal{D}^{(2)} P \right)}} \right).$$

This completes the proof. \blacksquare

Appendix M. Beyond the first dimension.

The consistency results discussed previously hinge on the assumption that the mirror is asymptotically piecewise linear in the first dimension, with the remaining dimensions carrying negligible signal. However, as observed in Fig 2.2, the changepoints are also detectable in

higher dimensions. To see this more precisely, we revisit the distance matrix for Model 2.20. Recall in Lemma 2.21,

$$\left(\mathcal{D}_{\varphi_m}^{(2)}\right)_{i,j} = \begin{cases} \frac{p^2}{m^2}(i-j)^2 + \frac{p-p^2}{m^2}|i-j| & i, j < t_m^* \\ \left(\frac{p}{m}(t_m^* - i) + \frac{q}{m}(j - t_m^*)\right)^2 + \frac{p-p^2}{m^2}(t_m^* - i) + \frac{q-q^2}{m^2}(j - t_m^*) & i < t_m^* < j \\ \frac{q^2}{m^2}(j-i)^2 + \frac{q-q^2}{m^2}|i-j| & t_m^* < i, j. \end{cases}$$

To study the mirror of Model 2.20, we perform CMDS on this distance matrix, which amounts to taking an eigendecomposition of $-\frac{1}{2}P\mathcal{D}_{\varphi_m}^{(2)}P$. When m is large, this eigendecomposition can be approximated through the kernel method of [7], in which we consider a kernel function $\kappa^m(x, y)$ that provides a continuous-time analogue of the discrete distance matrix, and a double-centering operator that approximates the discrete centering with an integral.

To that end, set $t^* := \frac{t_m^*}{m}$. Define the corresponding kernel function $\kappa^m(x, y) : [0, 1]^2 \rightarrow \mathbb{R}$ as follows:

$$\kappa^m(x, y) = \begin{cases} p^2(x-y)^2 + \frac{p-p^2}{m}|x-y| & x, y < t^*. \\ \begin{aligned} &(t^* - x)^2 p^2 + \frac{p-p^2}{m}(t^* - x) + (y - t^*)^2 q^2 + \frac{q-q^2}{m}(y - t^*) + \\ &2pq(y - t^*)(t^* - x) \end{aligned} & x < t^* < y. \\ \begin{aligned} &(t^* - y)^2 p^2 + \frac{p-p^2}{m}(t^* - y) + (x - t^*)^2 q^2 + \frac{q-q^2}{m}(x - t^*) + \\ &2pq(x - t^*)(t^* - y) \end{aligned} & y < t^* < x. \\ q^2(x-y)^2 + \frac{q-q^2}{m}|x-y| & t^* < x, y. \end{cases}$$

and a double-centering operator \mathcal{DC} :

$$\mathcal{DC}[\kappa(x, y)] := \kappa(x, y) - \int_0^1 \kappa(x, y) dx - \int_0^1 \kappa(x, y) dy + \int_0^1 \int_0^1 \kappa(x, y) dx dy.$$

The continuous-time analogue of $P\mathcal{D}_{\varphi_m}^{(2)}P$ is $\mathcal{DC}[\kappa^m(x, y)]$, defined by

(M.1)

$$\mathcal{DC}[\kappa^m(x, y)] = \begin{cases} p^2 \left((2t_m^* - t_m^{*2}) (x + y) - 2xy \right) + \frac{p-p^2}{m} (|x - y| - x^2 - y^2 + x + y) + pq (1 - t_m^{*2}) (x + y) + c_1, & x, y < t_m^*; \\ -p^2 t_m^{*2} x - \frac{p-p^2}{m} x^2 + q^2 (t_m^* - 1)^2 y + \frac{q-q^2}{m} (2y - y^2) + pq (-2xy + (2t_m^* - t_m^{*2}) y + (-t_m^{*2} + 2t_m^* + 1) x) + c_2, & x < t_m^* < y; \\ -p^2 t_m^{*2} y - \frac{p-p^2}{m} y^2 + q^2 (t_m^* - 1)^2 x + \frac{q-q^2}{m} (2x - x^2) + pq (-2xy + (2t_m^* - t_m^{*2}) x + (-t_m^{*2} + 2t_m^* + 1) y) + c_2, & y < t_m^* < x; \\ q^2 \left((2t_m^* - t_m^{*2}) (x + y) - 2xy \right) + \frac{q-q^2}{m} (|x - y| - x^2 - y^2 + x + y) + pq (1 - t_m^{*2}) (x + y) + c_3, & x, y > t_m^*; \end{cases}$$

where c_1, c_2, c_3 are constants.

Observe that each of these kernels induces an associated integral operator $I_\kappa : L^2([0, 1]) \rightarrow L^2([0, 1])$ defined by

$$I_\kappa[f](x) = \int_0^1 \kappa(x, y) f(y) dy.$$

The κ_c^m kernel defined as $\kappa_c^m(x, y) := -\frac{1}{2} \mathcal{DC}[\kappa^m(x, y)]$ approximates our doubly-centered matrix in that the entrywise errors decay with m , as the following lemma demonstrates.

Lemma M.1. *With κ_c^m defined as $\kappa_c^m(x, y) := -\frac{1}{2} \mathcal{DC}[\kappa^m(x, y)]$, define a matrix S with its i, j entry as:*

$$S_{i,j} := \kappa_c^m \left(\frac{i}{m}, \frac{j}{m} \right).$$

Then for large m we have

$$\max_{1 \leq i \leq m, 1 \leq j \leq m} \left| S_{i,j} - \left(-\frac{1}{2} P \mathcal{D}_{\varphi_m}^{(2)} P \right)_{i,j} \right| \sim \Theta \left(\frac{1}{m} \right).$$

This lemma is proved in Section N. For an integral operator I_κ , its eigenvalues λ and eigenfunctions $f \in L^2([0, 1])$ satisfy

$$I_\kappa[f](x) = \lambda f(x) \quad \text{for all } x \in [0, 1].$$

The following theorem gives an explicit form for the eigenfunctions of the integral operator $I_{\kappa_c^m}$.

Theorem M.2. *Let the kernel function $\kappa_c^m(x, y) = -\frac{1}{2} \mathcal{DC}[\kappa^m(x, y)]$, where $\mathcal{DC}[\kappa^m(x, y)]$ is defined in Equation M.1. Suppose that the eigenvalues of its corresponding integral $I_{\kappa_c^m}$*

operator are positive. Then any eigenfunction of I_{κ^m} must take the following form:

$$k(x) = \begin{cases} A_{\text{pre}} \cos\left(\sqrt{\frac{p(1-p)}{m\lambda}}x\right) + B_{\text{pre}} \sin\left(\sqrt{\frac{p(1-p)}{m\lambda}}x\right) & \text{for } x \leq t^* \\ A_{\text{post}} \cos\left(\sqrt{\frac{q(1-q)}{m\lambda}}x\right) + B_{\text{post}} \sin\left(\sqrt{\frac{q(1-q)}{m\lambda}}x\right) & \text{for } x > t^*, \end{cases}$$

where λ , A_{pre} , B_{pre} and A_{post} , B_{post} are real numbers and satisfy $\int_0^1 k(t)dt = 0$, $\int_0^1 k^2(t)dt = 1$. Thus, the approximated mirror for [Model 2.20](#) will be $k(x)$ scaled by the square root of the eigenvalues.

Determining λ , A_{pre} , B_{pre} and A_{post} , B_{post} requires the solution of an especially complicated equation, but an explicit solution is unnecessary. Rather, [Theorem M.2](#) demonstrates that there is a change in frequency at t^* in all eigenfunctions, making the estimated eigenvectors in all dimensions a useful object of study for changepoint localization.

As shown in [Figure 3.1](#), the first dimension of the estimated mirror exhibits approximate piecewise linearity with a slope change at t^* . The second and third dimensions also exhibit a change in behavior at t^* , where the frequency of the cosine and sine curves change abruptly. This suggests a robustness to misspecification of embedding dimension: if we choose too large a dimension for the estimated mirror, the corresponding eigenfunctions still buttress the case for a changepoint at t^* , but estimates of these eigenfunctions become increasingly variable. This bias-variance tradeoff is illustrated in [Section 3.3](#).

Appendix N. Proof of Lemma M.1.

Proof. Consider the function $\kappa^m(x, y)$ as defined in [Section M](#). Note this function is bounded on $[0, 1] \times [0, 1]$. Putting $x_i = i/m$, we observe

$$\kappa^m(x_i, x_j) = (\mathcal{D}_{\varphi_m}^{(2)})_{i,j}.$$

Since $P = I - \frac{J}{m}$ and J is an all ones matrix, $P\mathcal{D}_{\varphi_m}^{(2)}P = \mathcal{D}_{\varphi_m}^{(2)} - \frac{1}{m}J\mathcal{D}_{\varphi_m}^{(2)} - \frac{1}{m}\mathcal{D}_{\varphi_m}^{(2)}J + \frac{1}{m^2}J\mathcal{D}_{\varphi_m}^{(2)}J$.

Recall that when approximating the Riemann integral by the Riemann sum computed at the right endpoint of a given partition, the following bound holds for the error.

Lemma N.1 (Right hand rule error bound for numerical integration). Suppose that $f(x)$ is differentiable on $[a, b]$ and $|f'(x)| \leq K_1$. Then

$$\int_a^b f(x) dx = \sum_{i=1}^m \frac{b-a}{m} f\left(\frac{i}{m}\right) + E_R \quad \text{where} \quad |E_R| \leq \frac{K_1(b-a)^2}{2m} \quad K_1 = \max_{x \in [a,b]} |f'(x)|.$$

We find

$$\left(\frac{1}{m}J\mathcal{D}_{\varphi}^{(2)}\right)_{i,j} = \sum_{t=1}^m \frac{1}{m} \left(\mathcal{D}_{\varphi}^{(2)}\right)_{t,j} = \sum_{t=1}^m \frac{1}{m} \kappa^m\left(\frac{t}{m}, x_j\right),$$

and

$$\begin{aligned} \sum_{t=1}^m \frac{1}{m} \kappa^m\left(\frac{t}{m}, x_j\right) &= \sum_{t=1}^{t_m^*} \frac{1}{m} \kappa^m\left(\frac{t}{m}, x_j\right) + \sum_{t=t_m^*+1}^m \frac{1}{m} \kappa^m\left(\frac{t}{m}, x_j\right) \\ &= \int_0^{t^*} \kappa^m(x, x_j) dx + R_{x_j} + \int_{t^*}^1 \kappa^m(x, x_j) dx + R'_{x_j}, \end{aligned}$$

where R_{x_j} is the error in approximating the first integral by the first sum, and R'_{x_j} is the error in approximating the second integral by the second sum.

Note here we apply the right hand rule error bound because $\kappa^m(x, y)$ is differentiable with respect to x on $[0, t^*]$ for any fixed $y \in [0, 1]$ and differentiable with respect to x on $[t^*, 1]$ for any fixed $y \in [0, 1]$. In addition, the derivative $\frac{d\kappa^m(x, y)}{dx}$ on $x \in [0, t^*]$ is bounded for any $y \in [0, 1]$; the same holds for $\frac{d\kappa^m(x, y)}{dx}$ on $x \in [t^*, 1]$. Thus by [Lemma N.1](#) we conclude that

$$R_{x_j} \leq \frac{\max_{x \in [0, t^*]} \left| \frac{d\kappa^m(x, y)}{dx} \right|}{2m} \leq \frac{\max_{y \in [0, 1]} \max_{x \in [0, t^*]} \left| \frac{d\kappa^m(x, y)}{dx} \right|}{2m} \leq \frac{C}{m} \quad \text{for } x_j \in [0, 1].$$

The analogous bound holds for R'_{x_j} . Together, we have an uniform upper bound for the error in the right-hand Riemann sum; namely for every $x_j \in [0, 1]$,

$$\sum_{t=1}^m \frac{1}{m} \kappa \left(\frac{t}{m}, x_j \right) = \int_0^1 \kappa(x, x_j) dx + R^{(1)} \quad \text{where} \quad |R^{(1)}| \sim O \left(\frac{1}{m} \right).$$

Note that

$$\left(\frac{1}{m} \mathcal{D}_{\varphi}^{(2)} J \right)_{i,j} = \sum_{t=1}^m \frac{1}{m} \left(\mathcal{D}_{\varphi}^{(2)} \right)_{i,t} = \sum_{t=1}^m \frac{1}{m} \kappa \left(x_i, \frac{t}{m} \right),$$

and since $\kappa^m(x, y)$ is symmetric, we have that for every $x_i \in [0, 1]$,

$$\sum_{t=1}^m \frac{1}{m} \kappa^m \left(x_i, \frac{t}{m} \right) = \int_0^1 \kappa^m(x_i, x) dx + R^{(2)} \quad \text{where} \quad |R^{(2)}| \sim O \left(\frac{1}{m} \right).$$

Now recall that

$$\left(\frac{1}{m^2} J \mathcal{D}_{\varphi_m}^{(2)} J \right)_{i,j} = \sum_{t'=1}^m \sum_{t=1}^m \frac{1}{m^2} \left(\mathcal{D}_{\varphi_m}^{(2)} \right)_{t',t} = \sum_{t'=1}^m \sum_{t=1}^m \frac{1}{m^2} \kappa \left(\frac{t'}{m}, \frac{t}{m} \right),$$

and thus

$$\begin{aligned} \sum_{t'=1}^m \sum_{t=1}^m \frac{1}{m^2} \kappa^m \left(\frac{t'}{m}, \frac{t}{m} \right) &= \sum_{t'=1}^m \frac{1}{m} \left(\sum_{t=1}^m \frac{1}{m} \kappa^m \left(x_{t'}, \frac{t}{m} \right) \right) \\ &= \sum_{t'=1}^m \frac{1}{m} \left(\int_0^1 \kappa(x_{t'}, y) dy + R^{(2)} \right) \\ &= \sum_{t'=1}^m \frac{1}{m} \int_0^1 \kappa^m(x_{t'}, y) dy + \sum_{t'=1}^m \frac{1}{m} R^{(2)} \\ &= \int_0^1 \int_0^1 \kappa(x, y) dx dy + R^{(3)} + R^{(2)} \\ \text{where} \quad |R^{(3)}| &\leq \frac{1}{2m} \max_{x \in [0, 1]} \left| \frac{d}{dx} \int_0^1 \kappa^m(x, y) dy \right| \sim O \left(\frac{1}{m} \right). \end{aligned}$$

Then for any $i, j \in \{1, 2, \dots, m\}$:

$$\begin{aligned} \left(-\frac{1}{2} P \mathcal{D}_{\varphi_m}^{(2)} P \right)_{i,j} &= -\frac{1}{2} \left(\mathcal{D}_{\varphi_m}^{(2)} - \frac{1}{m} J \mathcal{D}_{\varphi_m}^{(2)} - \frac{1}{m} \mathcal{D}_{\varphi_m}^{(2)} J + \frac{1}{m^2} J \mathcal{D}_{\varphi_m}^{(2)} J \right)_{i,j} \\ &= -\frac{1}{2} \left[\kappa^m(x_i, x_j) - \int_0^1 \kappa^m(x, x_j) dx \right. \\ &\quad \left. - \int_0^1 \kappa^m(x_i, y) dy + \int_0^1 \int_0^1 \kappa^m(x, y) dx dy \right. \\ &\quad \left. - R^{(1)} - R^{(2)} + R^{(3)} + R^{(2)} \right]. \end{aligned}$$

Because

$$\kappa_c^m(x_i, x_j) = -\frac{1}{2} \left[\kappa(x_i, x_j) - \int_0^1 \kappa^m(x, x_j) dx - \int_0^1 \kappa(x_i, y) dy + \int_0^1 \int_0^1 \kappa(x, y)^m dx dy \right],$$

we derive

$$\left| \left(-\frac{1}{2} P \mathcal{D}_{\varphi}^{(2)} P \right)_{i,j} - \kappa_c^m(x_i, x_j) \right| = \frac{1}{2} \left| -R^{(1)} - R^{(2)} + R^{(3)} + R^{(2)} \right| \sim O\left(\frac{1}{m}\right) \quad \forall x_i, x_j \in [0, 1].$$

This completes the proof. ■

Appendix O. Proof of Theorem M.2.

Proof. Consider a function $f(y) = g(y)$ for $y \leq t^*$, $f(y) = h(y)$ for $y > t^*$, where $g(t^*) = h(t^*)$. If f is an eigenvector of the integral operator induced by κ_c^m , then

$$\begin{aligned} & -\frac{1}{2} \int_0^1 \mathcal{DC}[\kappa^m(x, y)] f(y) dy = \lambda f(x), \text{ so} \\ (x < t^*) : & \int_0^{t^*} \mathcal{DC}[\kappa^m(x, y)] g(y) dy + \int_{t^*}^1 \mathcal{DC}[\kappa^m(x, y)] h(y) dy = -2\lambda g(x) \\ (x > t^*) : & \int_0^{t^*} \mathcal{DC}[\kappa^m(x, y)] g(y) dy + \int_{t^*}^1 \mathcal{DC}[\kappa^m(x, y)] h(y) dy = -2\lambda h(x). \end{aligned}$$

We compute the second derivative with respect to x for each of the two cases; specifically

$x < t^*$ and $x > t^*$:

$$\begin{aligned}
(x < t^*) : \quad & \frac{\partial^2}{\partial x^2} \int_0^{t^*} \mathcal{DC}[\kappa^m(x, y)]g(y) \, dy = \int_0^{t^*} \frac{p-p^2}{m}(-2)g(y) \, dy \\
& + \frac{\partial^2}{\partial x^2} \int_0^x \frac{p-p^2}{m}(x-y)g(y) \, dy + \int_x^{t^*} \frac{p-p^2}{m}(y-x)g(y) \, dy \\
& = \frac{p-p^2}{m}(-2)[G(t^*)-G(0)] + \frac{\partial}{\partial x} \int_0^x \frac{p-p^2}{m}g(y) \, dy + \int_x^{t^*} \frac{p-p^2}{m}(-1)g(y) \, dy \\
& = \frac{p-p^2}{m} [(-2)(G(t^*)-G(0))+2g(x)]. \\
(x < t^*) : \quad & \frac{\partial^2}{\partial x^2} \int_{t^*}^1 \mathcal{DC}[\kappa^m(x, y)]h(y) \, dy \\
& = \int_{t^*}^1 \frac{p-p^2}{m}(-2)h(y) \, dy \\
& = \frac{p-p^2}{m}(-2)[H(1)-H(t^*)].
\end{aligned}$$

We observe that $G(t^*) - G(0) + H(1) - H(t^*) = \int_0^{t^*} g(y) \, dy + \int_{t^*}^1 h(y) \, dy = \int_0^1 f(y) \, dy = 0$, so the first equation (for $x < t^*$) becomes

$$\frac{2p(1-p)}{m}g(x) = -2\lambda g''(x).$$

For the second equation,

$$\begin{aligned}
(x > t^*) : \quad & \frac{\partial^2}{\partial x^2} \int_0^{t^*} \mathcal{DC}[\kappa^m(x, y)]g(y) \, dy = \int_0^{t^*} \frac{q-q^2}{m}(-2)g(y) \, dy, \\
& = \frac{q-q^2}{m}(-2)[G(t^*) - G(0)]. \\
(x > t^*) : \quad & \frac{\partial^2}{\partial x^2} \int_{t^*}^1 \mathcal{DC}[\kappa^m(x, y)]h(y) \, dy \\
& = \int_{t^*}^1 \frac{q-q^2}{m}(-2)h(y) \, dy \\
& + \frac{\partial^2}{\partial x^2} \int_{t^*}^x \frac{q-q^2}{m}(x-y)h(y) \, dy + \int_x^1 \frac{q-q^2}{m}(y-x)h(y) \, dy \\
& = \frac{q-q^2}{m}(-2)[H(1) - H(t^*)] \\
& + \frac{\partial}{\partial x} \int_{t^*}^x \frac{q-q^2}{m}h(y) \, dy + \int_x^1 \frac{q-q^2}{m}(-1)h(y) \, dy \\
& = \frac{q-q^2}{m} [(-2)(H(1) - H(t^*)) + 2h(x)].
\end{aligned}$$

Again applying the condition $\int_0^1 f(y) dy = 0$, the equation for $x > t^*$ reads

$$\frac{2q(1-q)}{m}h(x) = -2\lambda h''(x).$$

Assuming $\lambda > 0$, the solutions to the differential equation for g must have the form e^{rx} where r is a root of the equation $r^2 + \frac{p(1-p)}{m\lambda} = 0$. In other words, $r = \pm i\sqrt{\frac{p(1-p)}{m\lambda}}$ for $\lambda > 0$. Arguing similarly for h , we see that the solutions must have the form

$$\begin{aligned} g(x) &= A_g \cos\left(\sqrt{\frac{p(1-p)}{m\lambda}}x\right) + B_g \sin\left(\sqrt{\frac{p(1-p)}{m\lambda}}x\right) \\ h(x) &= A_h \cos\left(\sqrt{\frac{q(1-q)}{m\lambda}}x\right) + B_h \sin\left(\sqrt{\frac{q(1-q)}{m\lambda}}x\right). \end{aligned} \quad \blacksquare$$